Fuel Cycle Design and Analysis of SABR: Subrcritical Advanced Burner Reactor

A Thesis

Presented to

The Academic Faculty

By

Christopher M. Sommer

In Partial Fulfillment

of the Requirements for the Degree

Master of Science in Nuclear Engineering

Georgia Institute of Technology

August 2008

Fuel Cycle Design and Analysis of SABR: Subrcritical Advanced Burner Reactor

Approved by:

Dr. Wilfred van Rooijen, Advisor
School of Nuclear and Radiological Engineering
Georgia Institute of Technology

Dr. Weston M. Stacey
School of Nuclear and Radiological Engineering
Georgia Institute of Technology

Dr. Nolan Hertel
School of Nuclear and Radiological Engineering
Georgia Institute of Technology

Date Approved: June 6, 2008

Acknowledgements

I would like to thank my advisor Dr. Wilfred van Rooijen for his guidance and support. I would also like to thank my committee members Dr. Weston Stacey and Dr. Nolan Hertel for their help on this project. I want to express my gratitude to the Department of Energy especially the Advanced Fuel Cycle Initiative for funding my research. I also would like to thank my parents for their love and support. Finally, thanks to Becky for her continuous love and support.

Table of Contents

List of Tables

List of Figures

Summary

Various fuel cycles for a sodium-cooled, subcritical, fast reactor with a fusion neutron source for the transmutation of light water reactor spent fuel have been analyzed. All fuel cycles were 4-batch, and all but one were constrained by a total fuel residence time consistent with a 200 dpa clad and structure materials damage limit. The objective of this study was to achieve greater than 90% burn up of the transuranics from the spent fuel.

The first two fuel cycle scenarios (A and B) examined the difference between in-to-out and out-to-in fuel shuffling for once-through fuel cycles, and the third scenario (C) examined the effect of a design variation on power flattening. The fourth fuel cycle (D) examined the achievement of greater than 90% TRU burnup in a once-through fuel cycle, assuming the development of an advanced structural material that could withstand the associated radiation damage. Finally, the fifth fuel cycle (E) analysis, which is representative of the reference fuel cycle envisioned for advanced burner reactors (ABRs), examined the achievement of 90% TRU burnup by repeated reprocessing/recyling of the TRU fuel.

For the subcritical advanced burner reactor (SABR) design used in these analyses, the 200 dpa limit on structural material irradiation corresponded to about 24% burnup of the TRU fuel in one residence time in the reactor. Achieving greater than 90% TRU fuel burnup without reprocessing in a once-through cycle, in the event that an advanced structural material with sufficient radiation resistance were to be developed in the future, was found to be technologically feasible but unattractive because of the highly non-uniform power distribution of the resulting low reactivity core in the one fuel cycle examined.

The reference fuel cycle, in which the TRU fuel was reprocessed, mixed with fresh TRU fuel, and recycled into the reactor after each 24% burnup residence time, achieved greater than 90% TRU burnup after 9 residence times. The fuel ultimately discharged to the high level waste repository (HLWR) was reduced relative to the original spent nuclear fuel (SNF) from which it was produced by 99% in integral decay heat at 100,000 years after discharge. The resulting repository volume required for the millennial storage of the fuel discharged from the SABR was calculated to be 1/130 the volume that would have been required to store the original SNF from which that fuel was made.

Chapter 1: Introduction

Commercial nuclear power production has created approximately 50,000 MT of Spent nuclear fuel (SNF) over the past 5 decades[1]. At the current rate of SNF production, 2,000 MT per year, the legislative cap on Yucca Mountain of 70,000 MT of SNF will be reached by 2018[2]. The predicted growth of SNF in the U.S., assuming a growth rate that maintains a market share of 20% electric power produced by nuclear power in the U.S, is shown in figure 1.

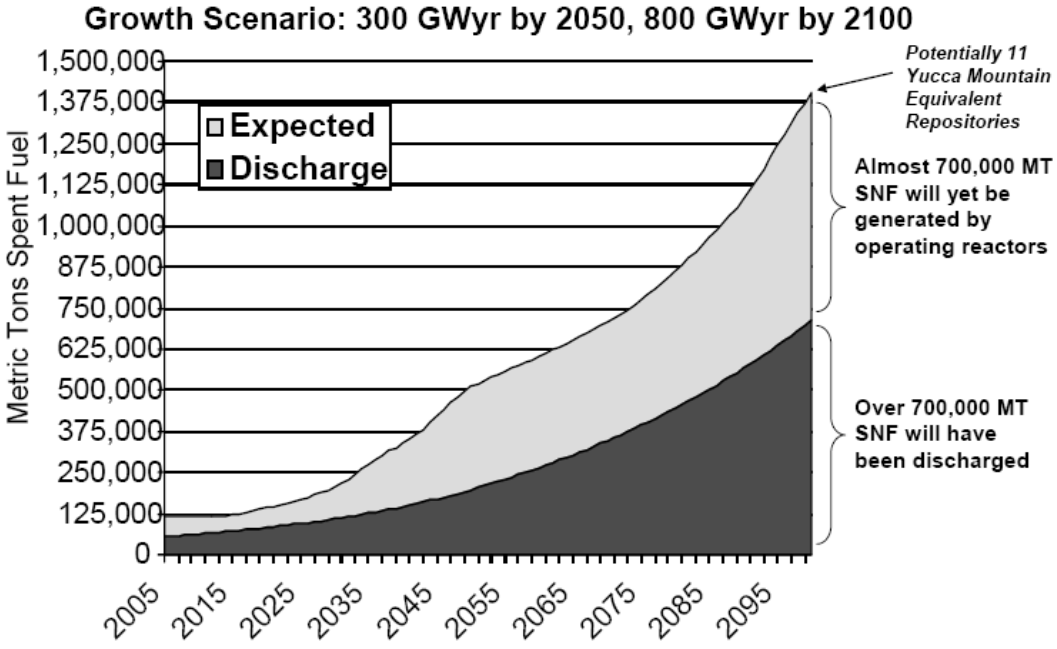

Figure 1: Storage requirements for a high level waste repository[3]

The Yucca Mountain project was established to create a permanent repository for SNF both from commercial nuclear power and government sources. If the legislative limit on Yucca Mountain is increased to the engineered limit there would be space for 120,000 MT of SNF and at the current production rate another repository would not be needed for another 25 years. This is assuming that the production of SNF from light water reactors (LWR) does not increase.

The capacity of Yucca Mountain is limited by the drift wall temperature at both emplacement and closure. Emplacement is the location in which the spent nuclear fuel is being transferred to in the repository. Closure is the time at which all of the SNF is in the repository and the repository is sealed off. The drifts are the location in which the spent nuclear fuel is stored in the repository. The temperature of the drift walls will increase over time due to the decay heat that is being generated by the waste being stored. Temperature is an issue because corrosion is accelerated at higher temperatures. There is no guarantee that water will not drip onto engineered parts creating brine and starting the corrosion process[4]. The repository is modeled as an adiabatic system such that deposited heat never leaves the system, resulting in a monotonic temperature increase with time after the repository is closed.

It is possible to increase the amount of space in Yucca Mountain by transmutation and separation of isotopes, as illustrated in Figure 2.

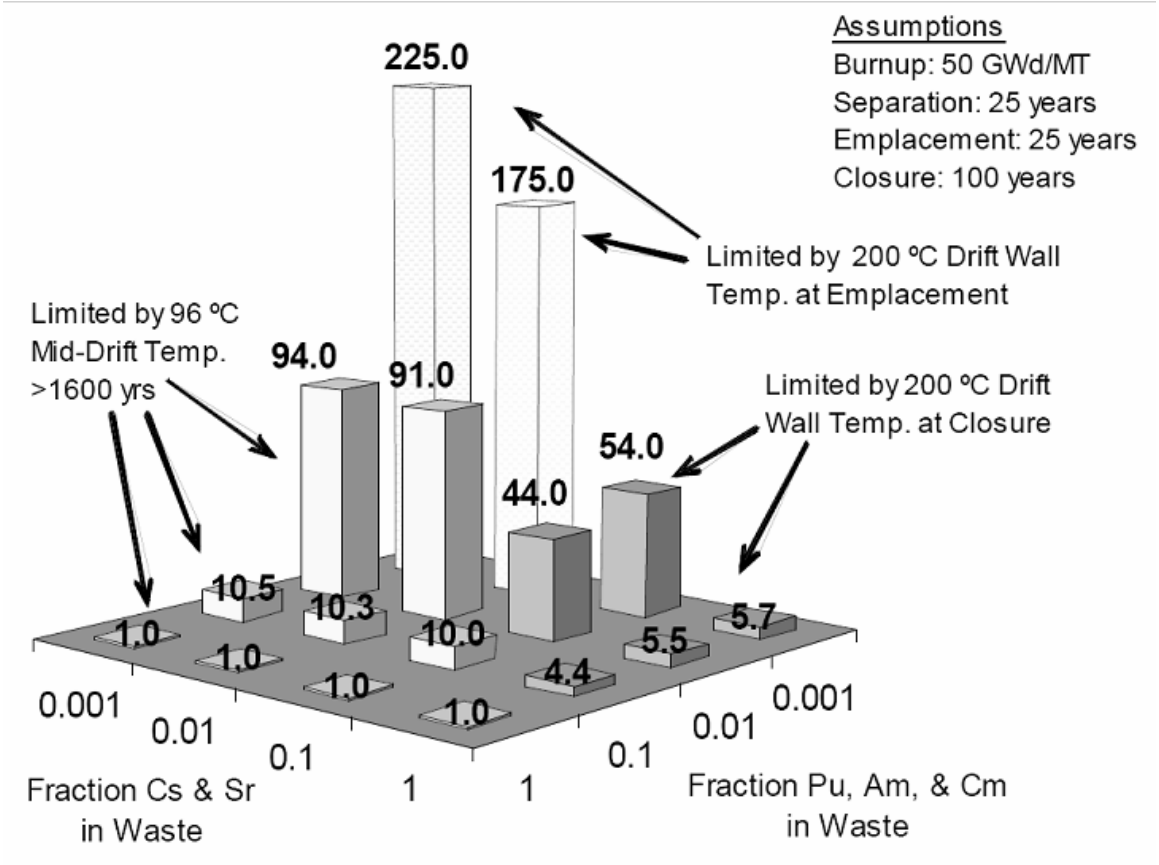

Figure 2: Transmutation and separation methods to increase the effective space of Yucca Mountain[5]

Figure 2 uses a two-fold approach to increasing the repository space. First, by separation of cesium and strontium, the short term heat load is greatly reduced, also causing a reduction in the integral heat load. Reducing the integral heat load is vital to increasing the effective amount of repository space. These two fission products produce a large amount of heat but decay away fairly quickly. Strontium 90, the largest heat producing isotope of strontium, has a half life of 29.1 years while cesium-137 has a half life of 30.2 years. This means that after 300 years (ten half lives) .1% of the strontium and cesium remain. There are two options for the separated cesium and strontium, they can either be stored separately until they decay away or another option is to use an accelerator to transmute these isotopes[6]. Second, transmutation of plutonium, americium, and curium can be utilized to reduce the repository space. Pu, Am, and Cm produce heat over hundreds of thousands of years. Not only are these isotopes producing heat on long time scales, their daughter products are also producing heat on long time scales. The transmutation of 90% of these actinide isotopes will lead to a ten-fold reduction in the required repository space for their storage in Yucca Mountain, as indicated in Figure 2.

With the introduction of the Global Nuclear Energy Partnership[7] (GNEP) and the energy policy act of 2005, the commercial nuclear power industry is experiencing a renaissance. According to the Nuclear Regulatory Commission (NRC), 32 new nuclear power plant applications are expected between 2007 and 2009[8]. These new power plants would come online before 2020. The addition of 32 nuclear power plants would increase the nuclear power production in the United States by approximately 33% thus increasing the SNF production by the same amount. Continuing with the once through cycle and a 33% increase in nuclear power the United States would need another repository the size of Yucca Mountain every 45 years if the repository is filled to the engineering limit.

A technical issue in the past, what to do with the SNF generated is now a political issue. A key component of GNEP is minimizing nuclear waste and in doing this making sure that proliferation is not an issue. Proliferation is the illicit use by third parties of nuclear materials to create a nuclear weapon. Light water reactors create plutonium as a by-product while creating energy. One method of reprocessing spent nuclear fuel, PUREX[9], isolates the plutonium and in doing this makes proliferation possible. Other reprocessing schemes such as UREX+[10] and pyroprocessing do not isolate the plutonium which makes these schemes more proliferation resistant. One way to minimize nuclear waste is to employ a multistep fuel cycle with fuel reprocessing and recycling instead of the once through fuel cycle that the United States currently employs. The multistep fuel cycle as envisioned by GNEP is shown below in figure 3.

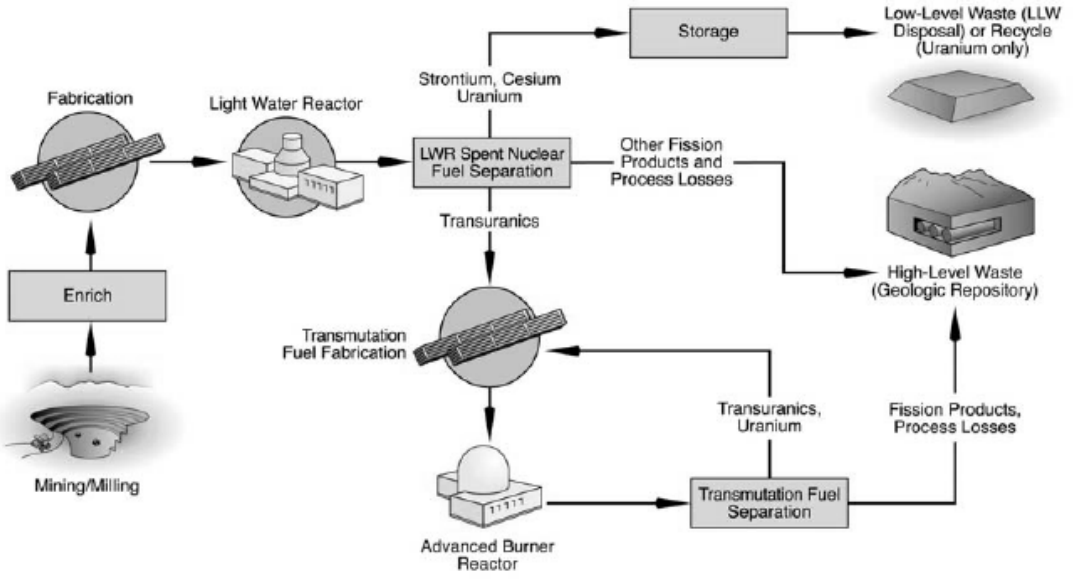

Figure 3: Multistep Fuel Cycle[11]

The multistep fuel cycle takes the transuranics from a light water reactor, fabricates these isotopes into new fuel and sends them to a fast reactor for transmutation. This serves two purposes, first it increases the energy utilization of the uranium mined from the ground. Second, it destroys the long lived radioactive waste so that it does not need to be stored in a repository, thus increasing the effective repository space. The once through cycle on the other hand is shown in figure 4:

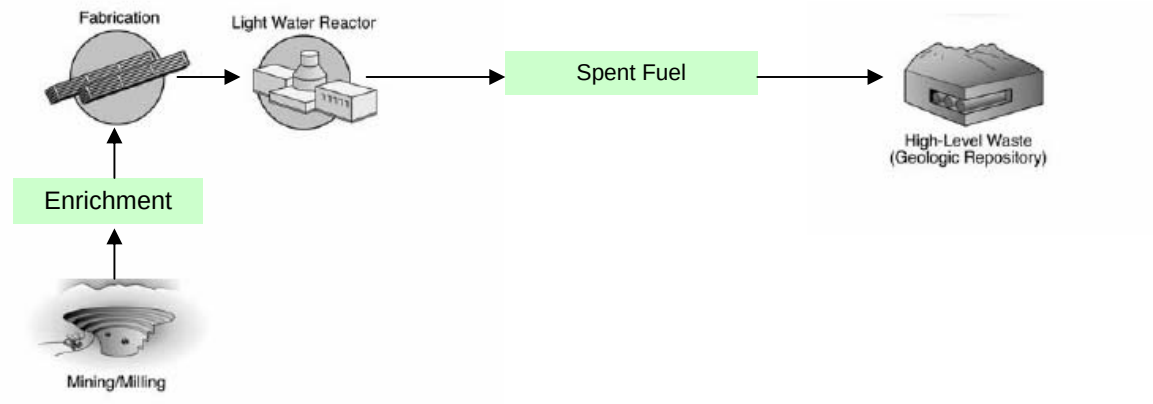

Figure 4: Once Through Cycle

The Department of Energy through the GNEP process is currently developing both separations technology for SNF and a fast reactor for the transmutation of SNF. The Advanced Burner Reactor (ABR) is a sodium cooled fast reactor that will be fueled with the SNF from light water reactors.

The transmutation rate for a given thermal power output would be maximized by using pure transuranic (TRU) fuel, with no uranium present. However, TRU fuel has a significantly smaller delayed neutron fraction, hence a significantly smaller margin to prompt critical, than ^{235}U. Moreover, the absence of ^{238}U in the fuel removes the source of the negative fuel Doppler Effect that would mitigate a power excursion. The use of subcritical reactors to increase the margin to prompt critical and to obtain larger burnup of the fuel before reprocessing has been suggested for the transmutation of SNF.

The fuel cycle for such a subcritical reactor option will be considered in this study. The use of subcritical reactors for transmutation of SNF provides for greater flexibility in the fuel cycle that is to be employed; maintaining criticality is no longer a constraint on the fuel cycle because as the fuel depletes and becomes less reactive the strength of the neutron source increases keeping the transmutation rate constant. The greater flexibility allowed by subcritical reactors could potentially produce a higher net transmutation rate per unit power and allow for greater destruction of high level waste than its critical counter part. Another advantage to subcritical operation is that of increased safety for the reactor. Transuranic (TRU) fuel has a smaller delayed neutron fraction. The smaller delayed neutron fraction is not a problem under subcritical operation because there is an increased margin to prompt criticality.

Currently a subcritical reactor for the transmutation of nuclear waste is being investigated at the Georgia Institute of Technology. This reactor, the Subcritical Advanced Burner Reactor (SABR)[12] is fueled by the TRU from current light water reactors and supplemented by a fusion neutron source. The fusion neutron source is modeled on the International Thermonuclear Experimental Reactor (ITER)[13] and is capable of producing 500 MW of fusion power. Due to the fact that ITER, which will serve as prototype for the neutron source, is scheduled to begin operation in 2017, SABR would be a second generation advanced burner reactor which could come online in about 2035.

The added flexibility of not having to maintain criticality in SABR gives many more options when exploring the potential fuel cycles for the reactor. This allows for longer fuel cycles because the fusion neutron source varies in strength. The increasing strength of the neutron source allows for greater subcritical operation while maintaining the same fission power level. It also allows for fuel cycles with a fuel composition that has a positive reactivity

feedback. The implications of a positive reactivity feedback can be mitigated in a subcritical reactor by the larger margin to prompt criticality. In the event of a transient the external source is shut off and the reactor shuts itself down because of subcritical operation. Finally, a subcritical reactor allows for operation with a very small delayed neutron fraction. The margin to prompt criticality is not a factor because of subcritical operation. Factors that need to be considered when implementing the fuel cycle are the power distribution in the reactor, the level of burnup that is obtained, tritium production to fuel the fusion source, and the amount of fusion power necessary to continue to burn the fuel at a given power level.

This thesis will focus on obtaining a fuel cycle that achieves a high burn up limited by radiation damage with a relatively flat power distribution. Further calculations will be done to ensure that enough tritium is bred for fueling the fusion neutron source. The limit on the fuel cycle for this reactor is the component lifetime due to radiation damage. Since the reactor employs a 14-MeV neutron source plus a fast fission spectrum the radiation damage per neutron is much higher than in a thermal reactor, therefore the fluence limits for the reactor are lower than that for a thermal reactor. Thus this study will focus on finding the optimal fuel cycle subject to the above constraints.

Chapter 2 Reactor Design

2.1 Configuration

SABR is a TRU-metal-fueled, sodium cooled, subcritical fast transmutation reactor driven by a D-T fusion neutron source. Shown in figure 5 is a simplified three dimensional model of the reactor, where figure 6 is a more complex model of the reactor. The fusion neutron source is surrounded on the outside by an annular fission core. Surrounding the fission core and the plasma there are tritium breeding blankets and many layers of shielding before the magnets that are used for the confinement of the plasma are reached.

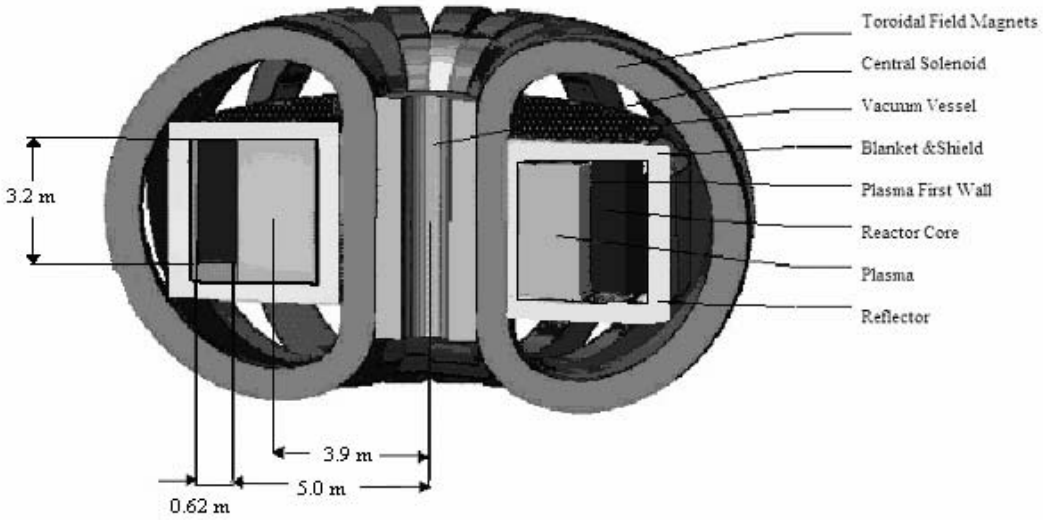

Figure 5: Configuration of SABR

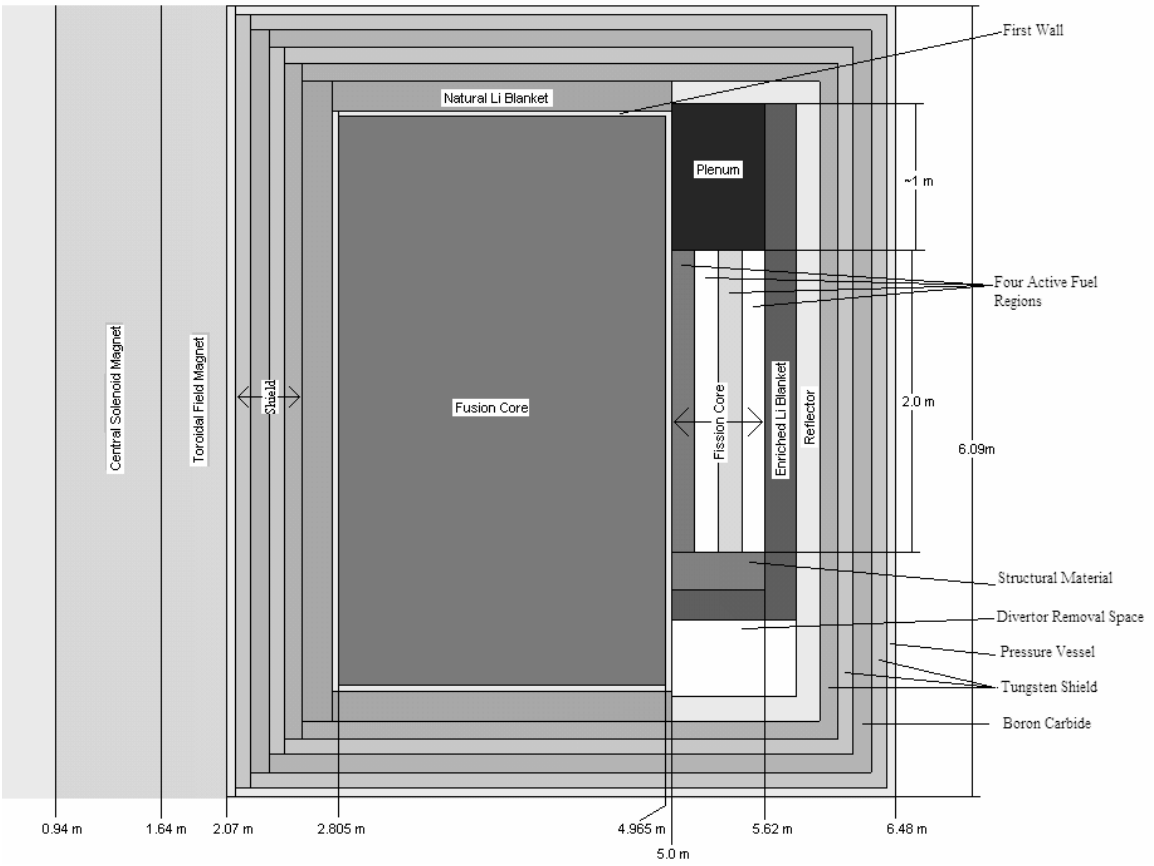

Figure 6: Detailed Cross Sectional Model of SABR

The fission core height of 3.2 m as show in figure 1 corresponds to the active length of the fuel rod 2.0 m, the plenum for fission gases of 1.0 m, and a top reflector of 20 cm. The fuel is arranged in hexagonal assemblies as shown in figure 7. Each fuel rod is 7.26 mm in diameter with an outer fuel diameter of 4 mm. The fuel is a metallic TRU/Zr slug, sodium bonded to an ODS steel for cladding. The core contains 918 hexagonal assemblies with each assembly containing 271 fuel rods.

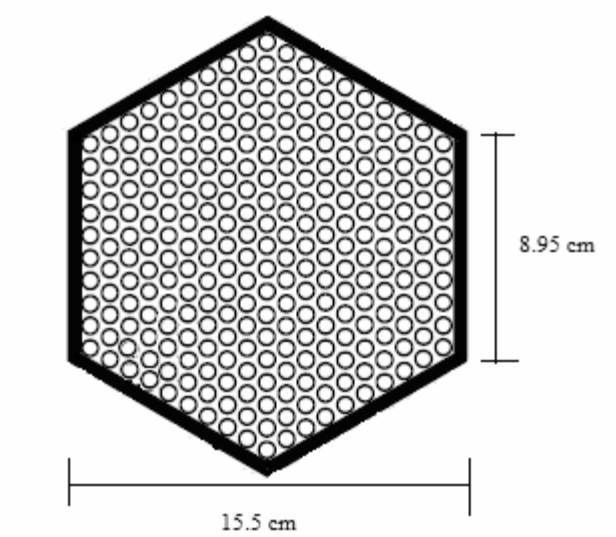

Figure 7: Hexagonal Fuel Assembly

2.2 Major parameters and materials

Table 1 shows the major parameters for SABR as well as the materials used in the design of SABR.

Table 1: Major Parameters for SABR

Fission Core	
Fission Power	3000 MWth
TRU Fuel Composition (wt./o)	Pu-40, Am-10, Np-10, Zr-40
Fuel Density	9.595 g/cm^3
Mass of TRU/ Fuel Material	36 MT/ 60 MT
Specific Power	83.3 kWth/ kg TRU
Maximum k_{eff}	0.95
Major Dimensions	R_{in} = 5 m, R_{out} = 5.62m, H_{active} =2 m
Fuel Pin	#=248,778, D_{fm} = 4.00 mm, D_o = 7.26 mm
Coolant mass flow rate, Temperature	$\dot{m}$ = 8700 kg/s, T_{in}/T_{out} = 377/650 °C
Power Density, Maximum T_{fuel} / T_{clad}	q'''=72.5 MW/m^3, $T_{fm,\ max}$ = 715°C, $T_{clad,max}$= 660°C
Linear Fuel Pin Power	6 kW/m
Clad, wire wrap, and flow tube	ODS ferritic steel, t = 0.5mm, 2.2mm, 2.0mm
Fuel/Clad,Gap,$LiNbO_3$/Structure/Coolant (v/o)	15/35/14/36
Fuel Assembly	#=918, Hexagonal, D_{flats}=15.5 cm, D_{side} = 8.95 cm
Reflector, Blanket, and Shield	
Reflector / Shield Materials	ODS Steel, Boron Carbide, Tungsten, Na cooled
Tritium Breeder	Li_4SiO_4
Combined Thickness	80 cm
Tritium Breeding Ratio	1.16
Coolant mass flow rate	$\dot{m}$ = 0.2 kg/sec
Min and Max blanket temperatures	T_{min}= 450°C/ T_{max}= 640°C
Plasma	
Plasma Current	8-10.0 MA
Fusion power/ neutron source rate	(50-500 MW)/(1.8e19 s^{-1} to 1.8e20 s^{-1})
Fusion gain ($Q_p = P_{fus}/P_{plasma\ heating}$)	180 MW_{th}/58 MW_{th} = 3.2
Superconducting Magnets	

Field CS, TFC, at center of plasma	13.5 T, 11.8 T, 5.9 T
TFC Magnet Dimensions	w = 5.4 m , h = 8.4 m, t_{rad} = 43 cm, t_{tor} = 36 cm
Divertor	
Materials	Tungsten, CuCrZr, Na cooled
Heat Flux	1-8 MW/m^2
Coolant mass flow rate	$\dot{m}$ = 0.09 kg/sec
First Wall	
Materials	Beryllium on ODS, Na cooled
Surface Area	223 m^2
Average Neutron wall load (14 MeV)	1.0 MW/m^2
Average Heat flux (500 MW)	0.25 MW/m^2
Coolant mass flow rate	$\dot{m}$ = 0.057 kg/sec

2.3 Fuel Element and Fuel Assembly Design

The fuel choices for SABR were broken up into two groups according to the reprocessing method required. The first group consisted of oxides, nitrides, and carbides which are reprocessed using aqueous methods. The second group consisted of metallic fuel forms and is reprocessed with a pyrometallurgic process. In the U.S the two fuel types being considered for transmutation in fast reactors with a high TRU content fuel are nitride and metallic fuel. Nitride fuels have been irradiated to 5.5% burnup in JMTR, while metallic fuels have reached 20% burnup in EBR-II[14]. The fuel choice for SABR was then made to be a metallic fuel.

The fuel as stated earlier is a TRU/Zr fuel element comprised of a weight percent composition of 40Zr-40Pu-10Np-10Am[15]. The isotopic composition of the fuel is given in table 2. The fuel was chosen due to its high thermal conductivity, high fission gas retention (ability for higher burn up), and the ability to contain a high density of actinides. Argonne National Lab (ANL) is currently undergoing research on this fuel composition and is among the fuel types being considered for the advanced burner reactor. Major parameters of both the fuel pin and the fuel assembly are given in table 3. Figure 8 shows a cross-sectional image of a fuel pin where figure 9 shows the 4 batch assembly layout.

Table 2: TRU Fuel Composition (ANL)[15]

	Mass percent
Isotope	Beginning of life (BOL)
^{237}Np	17.0
^{238}Pu	1.4
^{239}Pu	38.8
^{240}Pu	17.3
^{241}Pu	6.5
^{242}Pu	2.6
^{241}Am	13.6
^{243}Am	2.8

Table 3: Key Design Parameters of Fuel Pin and Assembly

Length rods (m)	3.2	Total pins in core	248778
Length of fuel material (m)	2	Diameter_Flats (cm)	15.5
Length of plenum (m)	1	Diameter_Points (cm)	17.9
Length of reflector (m)	0.2	Length of Side (cm)	8.95
Radius of fuel material (mm)	2	Pitch (mm)	9.41
Thickness of clad (mm)	0.5	Pitch-to-Diameter ratio	1.3
Thickness of Na gap (mm)	0.83	Total Assemblies	918
Thickness of $LiNbO_3$ (mm)	0.3	Pins per Assembly	271
Radius Rod w/clad (mm)	3.63	Flow Tube Thickness (mm)	2
Mass of fuel material per rod (g)	241	Wire Wrap Diameter (mm)	2.24
$Volume_{Plenum}$ / $Volume_{fm}$	1	Coolant Flow Area/ assy (m^2)	7.5

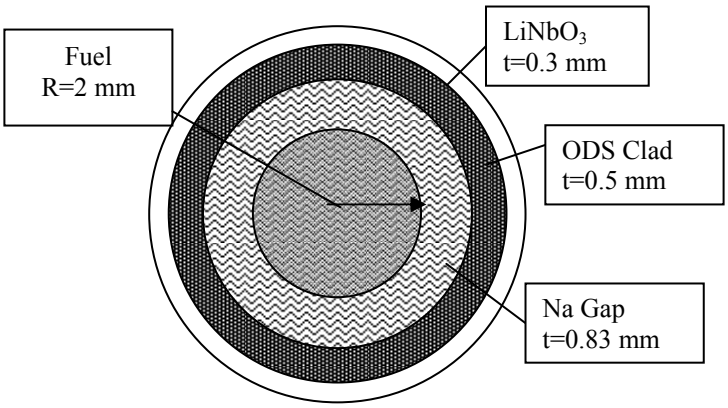

Figure 8: Cross Sectional View of Fuel Rod

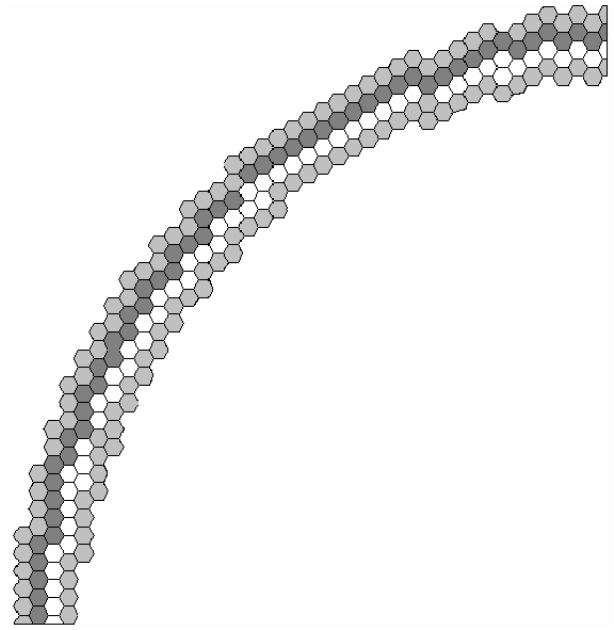

Figure 9: Four batch layout of Fuel Assemblies in SABR

2.4 Fuel Fabrication

Fabrication of the new fuel rods for SABR will be done via arc casting. Arc casting will also be used to fabricate the rods for the initial loading of SABR. Fabrication has only been done on the laboratory level and the procedure used is not believed to scale up to an industrial scale; therefore many batches will have to be processed and an automation sequence is necessary; the fabrication will be done remotely in a hot cell[16] . An assembly line feature would be used in the hot cell to ensure integrity of the casting and fabrication process. A flow sheet of the fabrication process is shown in figure 10.

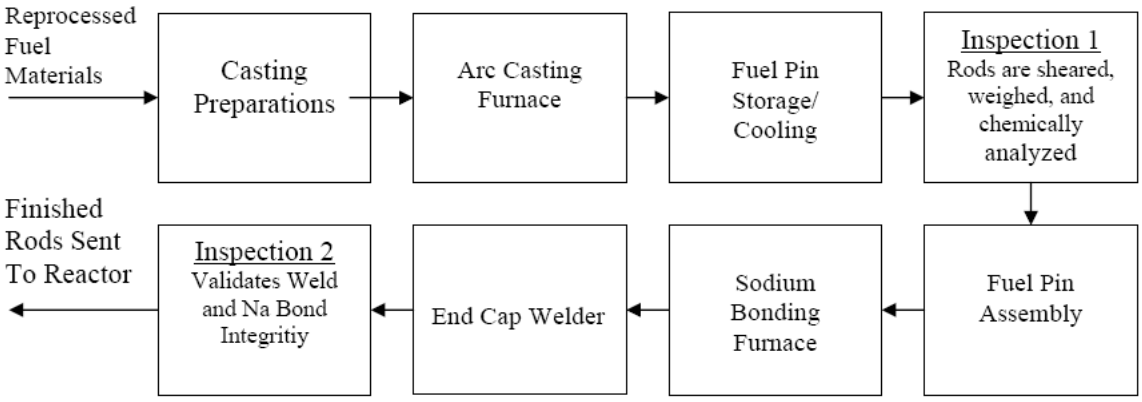

Figure 10: Fuel Fabrication Flow Chart

The amount of time it takes to fabricate a single batch of fuel is estimated at less than 4 hours with the majority of the time spent on the casting and the cooling of the fuel; while each batch is limited to a maximum mass of 3 kg due to criticality concerns[17]. Assuming two 8 hour shifts a day the amount of fuel rods that can be produced at one facility is 8760 kg/year, about 45% of the TRU generated by nuclear power plants annually in the U.S.[18].

2.5 Reprocessing

The reprocessing method of pyro-reprocessing was chosen based on the fuel choice of metallic fuel. The metallic fuel was chosen because of its proven high burnup capability in EBR-II[14]. Also current research into transmutation reactors with high actinide content in the fuel is being done with a metallic fuel[19]

There seem to be a couple advantages to pyrometallurgical reprocessing over an aqueous reprocessing system. First it is deemed to be proliferation resistant, because there are only two streams in the process: a fission product stream and a stream of minor actinides. Secondly it takes a much smaller facility for pyro-reprocessing, as compared to aqueous reprocessing, and therefore can be done on-site reducing overall costs and risk associated with the transportation of SNF[20.] Another advantage of pyro-reprocessing of metal fuel is that the product form of this method is metallic instead of an aqueous solution so there is no need to convert the product back into metal form for fabrication of fuel pins[21].

Pyrometallurgical reprocessing uses high-temperature chloride salts to melt the spent fuel, and then applies electro refining to separate the actinides and the fission products[22,23]. After the fuel is melted down it undergoes an oxidation process in which it is formed into a chloride complex. Following the oxidation stage a voltage is applied to electrodes and the highly reactive metals deposit themselves on the electrodes[24]. Figure 11 is a flow chart of the steps taken in pyro-reprocessing. For the fuel in SABR the reprocessing facility would start after oxide reduction since it is already a metallic fuel.

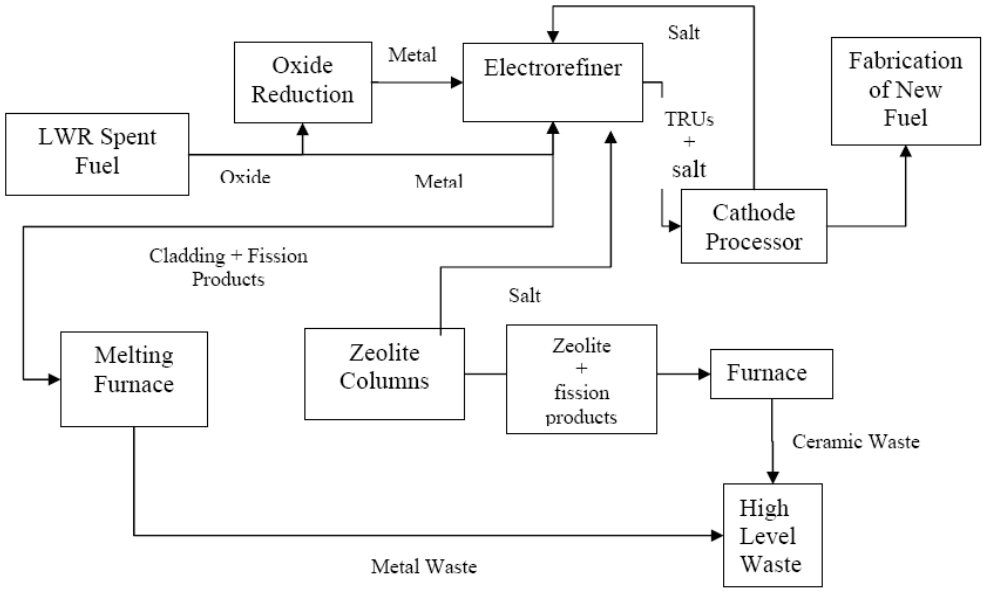

Figure 11: Pyrometallurgical Reprocessing flow chart

Even though pyro-reprocessing is an older technology it has only been used to make fuel on a limited basis for EBR I & II. Thus there is no industrial scale experience for reprocessing metallic fuel for fast reactors. Currently research and development is on going at Argonne National Lab into pyro-reprocessing[25].

2.5.1 Assumptions made in reprocessing of SABR Fuel

Since there is no industrial scale experience for reprocessing metal fuel several assumptions had to be made. The recovery rates and contamination rates for the minor actinides had to be estimated. Research at Argonne National Lab has estimated recovery rates of Np, Pu, Am, and Zr which is shown in table 4, but this is on a lab scale and there are no reports of contamination factors[19].

Table 4: Recovery Rates for Pyrometallurgical Reprocessing

Element	Estimated Recovery Rate (%)
Np	99.85
Pu	99.85
Am	99.97
Zr	99.95

This study uses a more conservative assumption when reprocessing the fuel. It is assumed that 99% of the actinides are recovered. In the minor actinide stream which is used to make the new fuel for SABR, it is assumed that 1% of the fission products that were produced in the fuel remain in this stream. Another assumption that was made was that of the mass flow rate through the process. It is not possible to scale up the batch sizes in reprocessing due to criticality concerns. One way to go from lab scale to industrial scale is to increase the number of stations which would increase the overall mass flow rate in the system but not the mass flow rate per station. It is assumed in this study that the reprocessing facility will have 311 days to reprocess one batch of fuel (6811 kg). This results in a mass flow rate of 21.9 kg/day and 7994 kg/yr. The amount of time for reprocessing was based on the flow rates for fuel fabrication, core loading time, fuel inspection time, the cool down time of the fuel and spent fuel pool capacity. Table 5 summarizes the mass flow rates for reprocessing and fuel fabrication for SABR.

Table 5: Reprocessing and Fuel Fabrication mass flow rates

Process	Time for Process (days)	Mass Flow Rate (kg/day)	Mass Flow Rate (kg/yr)
Inspection and Transportation	30	N/A	N/A
Reprocessing Fuel	311	21.9	7994
Fabrication	379	23.8	8687
Loading Core	30	N/A	N/A

2.6 Fusion Neutron Source

The fusion source for SABR is a D-T tokamak based on the source for the GCFTR-[26,36], which was a gas cooled subcritical fast transmutation reactor with a fusion neutron source previously investigated at Georgia Tech. The fusion source is capable of generating 500 MW of fusion power. In order to achieve the 500 MW of fusion power, the plasma requires external heating and current drive systems. There are six lower hybrid wave launchers with each wave launcher supplying about 20 MW of heating for the system and 1.5 MA of current drive.

2.7 Breeding Blanket Design

Tritium breeding is necessary in SABR because the fusion neutron source is fueled by a D-T plasma, $D + T \rightarrow {}^{4}He + n$. The tritium breeding blanket serves two purposes; primarily the blanket produces tritium for the fusion neutron source. Secondly, the blanket will reflect some of the neutrons that leak out of the fission core back into the core therefore acting as a reflector. Each breeding blanket located at the outer boundaries of the fusion core and fission core is made of Li_4SiO_4, ODS, and Na coolant. Lithium silicate was chosen because it has a high lithium atom density and low probability of the formation of hydroxides. The two breeding blankets are designed differently to accommodate the neutron energy spectrum that is leaving either the fusion core or the fission core depending on which region that blanket surrounds. Natural lithium is composed of two isotopes, ^{7}Li and ^{6}Li, with concentrations of 93% and 7%, respectively, in its natural state. Breeding tritium around the fusion core in a hard neutron spectrum natural lithium was used in the blanket due to the neutron absorption cross section for high energy neutrons in ^{7}Li. While the blanket that surrounds the fission core is enriched to 90% ^{6}Li because at lower energies ^{6}Li has a much larger neutron absorption cross section than ^{7}Li. These cross sections can be seen in figure 12 below.

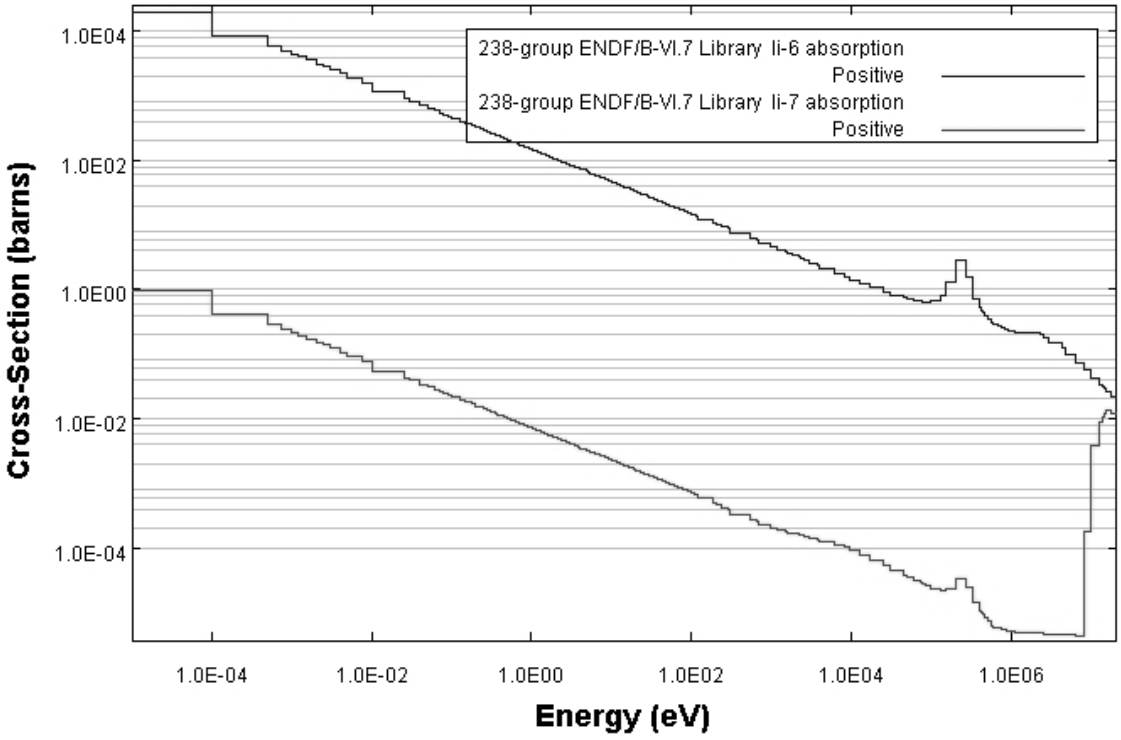

Figure 12: Absorption cross section comparison of ^{6}Li to ^{7}Li[27]

Tritium is removed from the blanket via a helium purge gas system. The breeding blankets contain channels for which helium flowed through to collect the tritium that is being produced. The helium tritium mixture is then processed where the tritium is separated from the helium and other impurities and then stored until it is injected into the plasma.

2.8 Electrical Performance

SABR produces 3,000 MW of thermal power in the fission core. The turbine converts the 3,000 MW_{th} to 1,049 MW_e. In calculating the electrical performance of SABR the power it takes to run the fusion neutron source, the coolant pumps, and the heaters. Less than 100 MW_e is used to power the heating and current drive of the fusion neutron source, 7.7 MW_e is used per pump, and the heaters use 30 MW_e. This results in a net electrical power of 911 MW_e and an overall efficiency of 30.4%.

Chapter 3 Theory

In this chapter the eigenvalue and flux calculations for critical and subcritical systems will be discussed. Secondly, the strength of the fusion neutron source and how it relates to the multiplication of the system is discussed. Next, the depletion equations and how these equations are coupled to the Boltzmann transport equation are shown. Finally, the governing equations for tritium breeding are discussed.

3.1 Core Theory

The governing equation for the eigenvalue and flux level in critical reactor calculations is the Boltzmann transport equation shown in equation 1:

$$[\hat{\Omega}\cdot\nabla+\sigma(\vec{r},E)]\Psi(\vec{r},\hat{\Omega},E)=\int dE'\int d\Omega'\sigma_s(\vec{r},E'\rightarrow E,\hat{\Omega}'\cdot\hat{\Omega})\Psi(\vec{r},\hat{\Omega}',E')+\frac{\chi(E)}{k}\int dE'\nu\sigma_f(\vec{r},E')\int d\Omega'\Psi(\vec{r},\hat{\Omega}',E') \quad (1)$$

where $\Psi(\vec{r},\hat{\Omega},E)$ is the angular flux, $\hat{\Omega}$ is the direction of neutron travel, $\sigma(\vec{r},E)$, is the total macroscopic cross section, $\sigma_s(\vec{r},E'\rightarrow E,\hat{\Omega}'\cdot\hat{\Omega})$ is the neutron scattering cross section, $\chi(E)$ is the fission spectrum, $\upsilon\sigma_f$ is the number of neutrons released per fission multiplied by the fission cross section, and k is the eigenvalue of the problem. The eigenvalue is used to determine if the system is critical. From a criticality standpoint any system can be made critical with this equation by adjusting the value of υ, the number of neutrons released per fission, between zero and infinity. If the system is subcritical, k<1, then the value of υ needs to be increased for the system to achieve criticality. If the system is critical, k=1, thus no adjustment to υ is necessary. For k >1, υ is too high and is adjusted so that fewer neutrons are released per fission, and the system is deemed supercritical. Summarizing:

k < 1, subcritical

k = 1, critical

k > 1, supercritical.

In the case of SABR k_{eff} is less than one and the reactor operates subcritically. In subcritical operation an external source of neutrons is necessary in order to find a steady state solution to the Boltzmann transport equation for any given power level. The steady-state Boltzmann equation with an external source is shown below:

$$[\hat{\Omega}\cdot\nabla+\sigma(\vec{r},E)]\Psi(\vec{r},\hat{\Omega},E)=\int dE'\int d\Omega'\sigma_s(\vec{r},E'\rightarrow E,\hat{\Omega}'\cdot\hat{\Omega})\Psi(\vec{r},\hat{\Omega}',E')+$$
$$\chi(E)\int dE'\nu\sigma_f(\vec{r},E')\int d\Omega\Psi(\vec{r},\hat{\Omega}',E')+q_{ex}(\vec{r},\hat{\Omega},E) \quad (2)$$

where all of the variables in the equation are the same as equation 1 and q_{ex} is an external source of neutrons at a given location, direction and energy. In the case of SABR they are 14.1 MeV neutrons from the D-T fusion neutron source.

3.2 Fusion Neutron Source Strength

The strength of the fusion neutron source is dependent on the desired power level of the reactor and k_m, the multiplication of the source neutrons. The derivation of this equation is shown starting with an integral neutron balance over the system as a starting point.

$$-\int\int_S J(\vec{E})\cdot\hat{n}dSdE-\int\int_V\Sigma_a(E)\phi(E)dVdE+\int\int_V\upsilon\Sigma_f(E)\phi(E)dVdE=-\int_V SdV \quad (3)$$

Equations 4 and 5 are substituted into equation 3 to yield equation 6. The fission and fusion power levels are represented by $P_{fission}$ and P_{fusion} respectively, while $E_{fission}$ and E_{fusion} represent the average energy released per fission and fusion event..

$$P_{fis}=\frac{1}{\upsilon}E_{fis}\int\int_V\upsilon\Sigma_f(E)\phi(E)dVdE\Rightarrow\int\int_V\upsilon\Sigma_f(E)\phi(E)dVdE=\upsilon\frac{P_{fission}}{E_{Fission}} \quad (4)$$

$$P_{fus}=E_{fus}\int_V S\cdot dV\Rightarrow\int_V S\cdot dV=\frac{P_{fusion}}{E_{fusion}} \quad (5)$$

$$-\int\int_S J(E)\cdot\hat{n}\cdot dSdE-\int\int_V\Sigma_a(E)\phi(E)\cdot dVdE+\upsilon\frac{P_{fission}}{E_{Fission}}=-\frac{P_{fusion}}{E_{fusion}} \quad (6)$$

Rearranging the terms on the left side of Equation 6 leads to Equation 7:

$$\left[\frac{-\left(\int\int_S J(E)\hat{n}\cdot dSdE+\int\int_V \Sigma_a(E)\phi(E)\cdot dVdE\right)}{\int\int_V \upsilon\Sigma_f(E)\phi(E)\cdot dVdE}+1\right]\cdot\upsilon\frac{P_{fission}}{E_{Fission}}=-\frac{P_{fusion}}{E_{fusion}} \tag{7}$$

Defining k_m as:

$$k_m=\frac{\int\int_V \upsilon\Sigma_f(E)\phi(E)\cdot dVdE}{\int\int_S J(E)\cdot\hat{n}\cdot dSdE+\int\int_V \Sigma_a(E)\phi(E)\cdot dVdE}=\frac{\text{Fission Neutron Production}}{\text{Total Neutron Absorprtion + Net Neutron Leakage}} \tag{8}$$

yields:

$$\left[\frac{1-k_m}{k_m}\right]\cdot\upsilon\frac{P_{fission}}{E_{Fission}}=-\frac{P_{fusion}}{E_{fusion}} \tag{9}$$

Equation 9 can then be rearranged to give Equation 10 which gives the required fusion power level as a function of the desired fission power and neutron multiplication level, k_m.

$$P_{fus}=\frac{E_{fus}}{E_{fis}}\nu\cdot\frac{(1-k_m)}{k_m}P_{fis} \tag{10}$$

The required increase is fusion power to maintain a constant fission power level is directly related to the decrease in the source multiplication due to burnup.

3.3 Depletion Equations

The transmutation equation for fuel depletion is shown below:

$$\frac{dN_i(r)}{dt}=-N_i\int\int_E \sigma_a(E)\Psi(r,\Omega,E)dEd\Omega-\lambda_i N_i(r)+\sum_{k\to i}\lambda_{k\to i}N_k(r)+$$
$$+\sum_l N_l(r)\int\int_E \sigma_{c,l\to i}(E)\Psi(r,\Omega,E)dEd\Omega+\int\int\sum_j y_{j,i}\sigma_{f,j}(E)N_j(r)\Psi(r,\Omega,E)dEd\Omega \tag{11}$$

where N_i is the number density of isotope i, σ_a is the microscopic absorption cross section, λ_i is the decay constant for isotope i, $\lambda_{k\to i}$ is the creation of isotope i from the decay of isotope k, $\sigma_{c,l\to i}$ is the creation of isotope i from a neutron capture in isotope l, σ_f is the fission cross section, $y_{j,i}$ is

the fission product yield of isotope i from a fission of isotope j and ψ is the angular flux. Taking the energy dependence out of the microscopic cross sections via equation 12:

$$\overline{\sigma(r)}_x = \frac{\int \int \sigma_x(E)\Psi(r,\Omega,E)d\Omega dE}{\int \int \Psi(r,\Omega,E)d\Omega dE} \qquad (12)$$

where $\sigma(r)_x$ is the microscopic cross section averaged over all energies and $\Psi(r,\Omega,E)$ is the solution of the Boltzmann equation and is a function of the number densities. The number densities solved for in the transmutation equations are a function of the angular flux and thus the two equations are coupled. Multiplying these microscopic cross sections by their respective number densities, N_i, yields the macroscopic cross section that is used in the Boltzmann transport equation. The transmutation equations show that fuel depletion is a function of space. Thus the angular flux and macroscopic cross section, σN, are calculated as a function of space. As the fuel depletes the macroscopic cross section for fission is reduced. The absorption cross section increases due to fission products being created in the reactor. The increase in the absorption cross section reduces k_m; therefore to maintain a constant fission power the fusion power must be increased. In SABR it is shown in equations 8 through 10 how the decrease in source multiplication increases the strength of the fusion neutron source.

3.4 Tritium Breeding

Tritium is a radioactive nuclide with a half life of 12.32 years and must be produced in order to fuel the fusion reaction. One method for production of tritium is via neutron capture in lithium. There are two isotopes of lithium in which a neutron is captured and tritium is produced ^{6}Li and ^{7}Li. The reactions for these two isotopes are shown below.

$$^6Li + n \rightarrow {}^4He + T \qquad (13)$$

$$^7Li + n \rightarrow {}^4He + T + n' \qquad (14)$$

Tritium production is governed by the production equation given in equation 15.

$$P_T = \sum_{Li-6,Li-7} \int \int \phi(r,E)\sigma_{(n,\alpha)}(E)N_{Li}\, dEdV \qquad (15)$$

P_T is the tritium production at a given time t, σ(n,α) is the microscopic (n, α) cross section, and N_{Li} is the number density of lithium. The destruction rate of tritium in the fusion reaction is dependent on the power level and is shown in equation 16.

$$D_T = \frac{P_{fusion}}{E_{fusion} * Q} \tag{16}$$

In this equation D_T is the destruction rate of tritium, P_{fusion} is the fusion power, E_{fusion} is the amount of energy released per tritium atom fused in MeV, and Q is the elementary charge. The production and destruction rate of tritium are coupled to each other through the fusion power and the resulting flux. The relationship between flux and fusion power is seen in equation 18, where f is a function.

$$\phi(r,E) = f(P_{fus}, k_m) \tag{17}$$

Equation 17 couples equations 6 and 7 showing that the destruction and production rate of tritium are not independent of one another.

The instantaneous rate of change in tritium atoms is shown in equation 18.

$$\frac{dN_T}{dt} = P_T(t) - D_T(t) - \lambda N_T(t) \tag{18}$$

Where N_t is the number density of tritium in the system. To calculate the amount of breeding, equation 18 is integrated over time and decay is taken into account. The discretization of this can be seen in section 4.5.

Chapter 4 Calculational Model

The calculations for the fuel cycle of SABR were done by employing the TRITON/NEWT[28,29] package from SCALE5.1[30] and the neutronics code EVENT[31]. A code, PERCOSET (Perl Coupling Of Scale and Event for Transmutation), was written to couple the cross section processing, the neutronics calculation and the depletion calculation in the fuel cycle. Figure 13 illustrates a flow chart for PERCOSET.

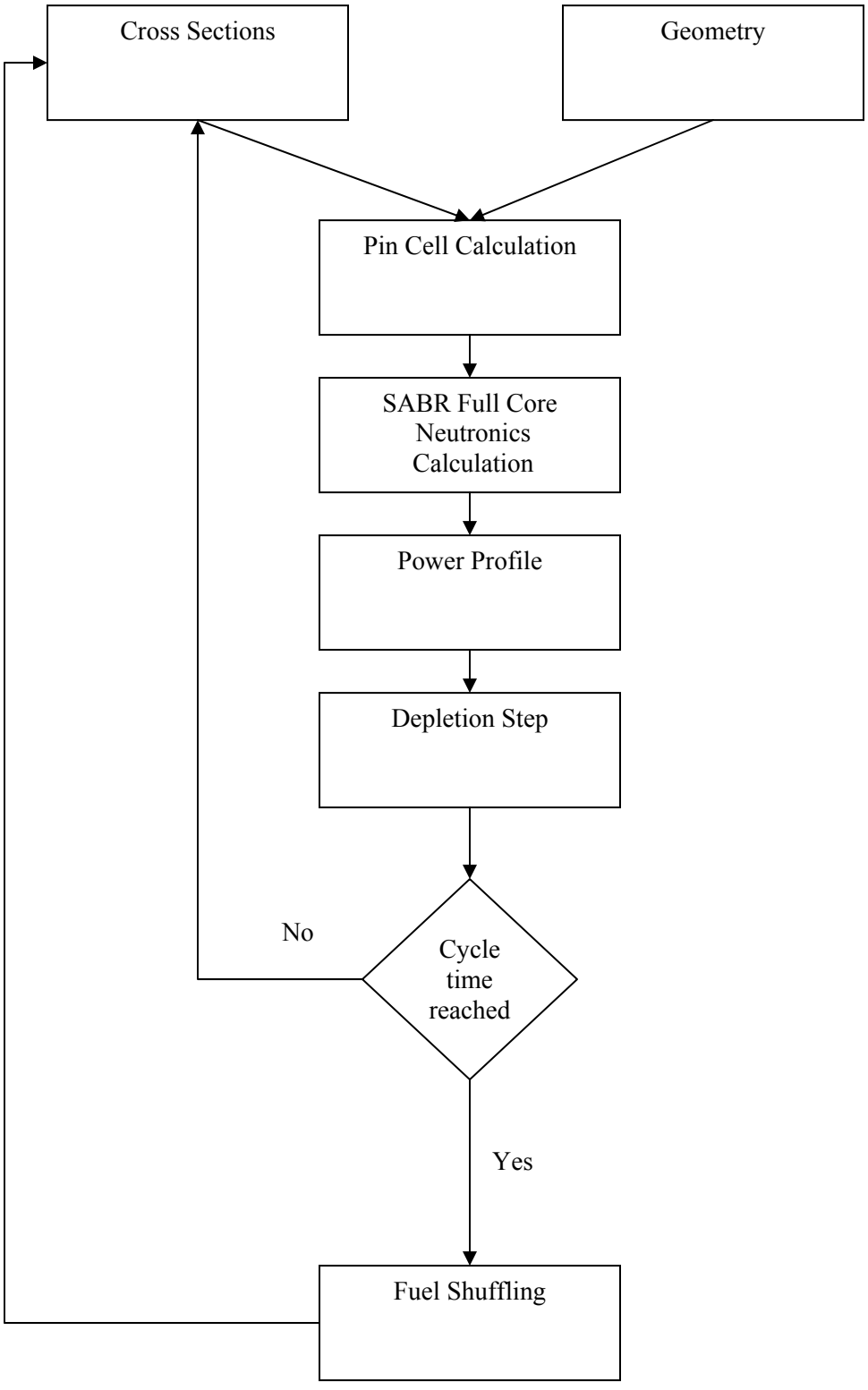

Figure 13: Flow Chart of PERCOSET

4.1 Pin Cell Calculation

Pin cell calculations are done in TRITON employing the T-NEWT capability. The pincell was modeled to include fuel, clad, and coolant. 27 group homogenized macroscopic cross sections are created for each material in the reactor. The 27 group structure was taken from NJOY[32] and is the ANL standard fast reactor set. These cross sections are post processed and put into a format for use by GEM and EVENT. The pin cell of figure 14 is a single pin from the fuel assembly of figure 7. In the pin cell calculation reflective boundary conditions were used to represent the rest of the fuel pins in an assembly.

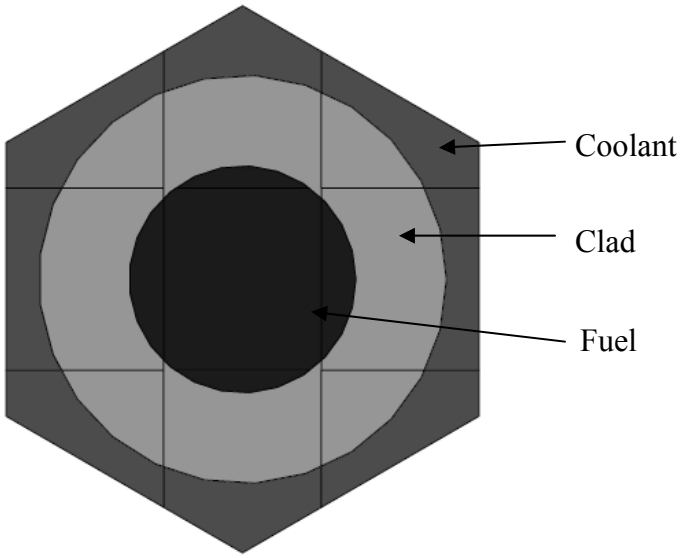

Figure 14: Pin cell model of a fuel pin

4.2 Neutronics Calculation

The neutronics calculation for SABR is done via GEM and EVENT. GEM is used to generate the geometry and key parameters for use by EVENT. EVENT is a three-dimensional transport code. EVENT uses the spherical harmonics method to solve the even parity transport equation. Assumptions that are made in the EVENT model are: the plasma is modeled as a void and the source neutrons are uniformly distributed over the volume of the first wall. Figure 6 in the reactor design chapter, shows a cross sectional model of SABR. The source neutrons in the

model are generated uniformly in the annular first wall which has a thickness of 3.5 cm. Modeling the plasma as a void is a valid assumption because it has a low density (1E-10 atoms/b*cm) making it neutronically inert.

4.3 Power Profile

A power profile is created for the depletion capability of PERCOSET. The power profile is created using the cross sections that were generated in the T-NEWT calculation and the flux profile from the neutronics calculation. The governing equation for calculating power from fluxes is:

$$P = \int\int \phi(r,E)\Sigma_f(r,E)E_{fis}\,dEdV \tag{19}$$

4.3.1 Power Equation

In multigroup theory equation 19 is discretized in energy groups. Furthermore in this reactor it is discretized over discrete volumes and the power calculation is done with the following equations:

$$P_{region} = \sum_{g=1}^{27} \phi_g \Sigma_{f,g} V E_{fis} \tag{20}$$

$$P = \sum_{region} P_{region} \tag{21}$$

These two equations result in a normalized power because the fluxes from EVENT are normalized. Equation 22 calculates the normalization factor ξ.

$$\xi = \frac{P}{P_0} \tag{22}$$

Where P is the desired power level of the reactor and P_0 is the normalized power obtained from EVENT. Obtaining a power profile is done by multiplying the normalization Factor by the power generated in each region (P_{region}).

4.4 Fuel Depletion

The depletion is done via TRITON/NEWT using a t-depletion (t-depl) sequence. The depletion is done on the pincell level and it is assumed that the depletion is the same in all pincells that are in the same region of the reactor. Each assembly is broken down into 4 regions for the neutronics calculation. Each region is 5 cm in radial thickness and 2 meters tall. Since there are 4 assemblies the core is broken down into 16 annular regions for both the neutronics and the depletion calculations. This assumption is valid because the regions are small for calculational purposes.

The same pincell that was modeled for the cross section processing is modeled and the fuel is depleted according to the power level obtained in the power profile section. The t-depl sequence inputs power in the units of MW/MTHM (Megawatts per metric ton heavy metal). Thus each region's power is divided by its volume and density of the region to obtain the appropriate numbers. SABR contains 36 MTHM and therefore the average depletion power in TRITON is 83.3 MW/MTHM.

4.5 Tritium Production

The Tritium Breeding blankets also need to be depleted and the breeding gain calculated. Discretization of equation 15 in section 3.4 in regards to energy and isotope type yields:

$$P_T(t) = \sum_{region} \sum_{I=Li6,Li7} \sum_{g=1}^{27} \phi_{g,region} \sigma_g^I(n,\alpha) N_{region}^I V_{region} \tag{23}$$

In calculating the breeding gain a linearization of equation 18 is done. This is done in the same manner as was done in a previous study by Maddox[33].

$$\frac{dN}{dt} = [P_{T1} + \frac{(P_{T2} - P_{T1}) * t}{C_{time}}] - [D_{T1} + \frac{(D_{T2} - D_{T1}) * t}{C_{time}}] - \lambda N_T(t) \tag{24}$$

P_{T1}, P_{T2}, D_{T1}, and D_{T2} are the beginning and end of cycle tritium production rates and beginning and end of cycle tritium destruction rates respectively.

Solving equation 24 for N_T(EOC) results in:

$$\begin{aligned} N_T(EOC) &= N_T(0) * e^{-C_{time}*\lambda} + \frac{P_{T1} - D_{T1}}{\lambda} * (1 - e^{-C_{time}*\lambda}) + \\ &+ \frac{[P_{T2} - P_{T1} + D_{T2} - D_{T1}]}{\lambda^2 * C_{time}} * (\lambda * C_{time} - 1 + e^{-C_{time}*\lambda}) \end{aligned} \tag{25}$$

When calculating the tritium breeding and therefore the tritium self sufficiency, a 90 day down time was assumed. The down time is the amount of time that occurs between cycles for maintenance and refueling. This is a conservative measure that takes into account problems during refueling since refueling outages should last approximately 30 days. Also the time it takes for the online gas purging of tritium to become available was estimated and taken into account when making the self sufficiency calculations. The amount of tritium needed at the beginning of cycle, $N_T(0)$, is calculated by equation 26.

$$N_T(0) = [D_{T1} + \frac{(D_{T2} - D_{T1}) * leadtime}{2 * C_{time}}] * leadtime \quad (26)$$

The "lead time" is the amount of time it takes for tritium from the online purge system to become available. Calculation of the amount of tritium present to start the fusion reaction after refueling is shown in equation 27, and equation 28 is what is necessary for tritium self sufficiency.

$$N_T(0') = N_T(EOC) * e^{-\lambda * downtime} \quad (27)$$

$$N_T(0') \geq N_T(0) \quad (28)$$

4.6 Fuel Shuffling

Finally, the fuel is shuffled between cycles. The fuel will be moved in one of two patterns: an In-to-Out pattern or an Out-to-In pattern. These patterns are discussed further in the results chapter.

4.7 PERCOSET

PERCOSET is needed to tie all of these individual modules together. Many of these modules incorporate smaller modules that PERCOSET ties together. This is necessary because TRITON/NEWT does not have the capability to do a source driven calculation and EVENT is not capable of depletion calculations. Following the flow chart in figure 13, the geometry of the pin cell and ENDF/BV 238 group cross sections in SCALE5.1 are combined into a pin cell calculation. PERCOSET creates a TRITON input to run a pincell calculation for each of the 16 fuel regions in the core, the reflector, axial and radial blankets, first wall and all of the shielding. The resulting cross sections are not in a format that can be used by EVENT; therefore PERCOSET uses AMPX[34] post processing modules in which these individual libraries are

combined into one master ANISN library that can be used by EVENT. EVENT calculates the flux profile using a P-1 approximation with 27 energy groups.

Once a master library has been generated the neutronics calculations are run in EVENT using an EVENT input file generated by PERCOSET. Two different calculations are done; first an eigenvalue calculation is done. EVENT calculates the k_{eff} of the system and if the system is supercritical the program gives an error message stating that the fuel compositions need to be changed because a fixed source calculation is not possible with a supercritical system. The results of the source driven calculation are the normalized fluxes that are used in generating the power profile for the depletion sequence.

The power profile generation sequence uses the fluxes generated from EVENT. This sequence is required because EVENT will not calculate a power profile which is needed for the t-depl sequence. Furthermore the power profile sequence uses the normalization factor to calculate the necessary fusion neutron source to operate at 3000 MW_{th}. Equation 29 is used to calculate the fusion power from the normalization factor.

$$P_{Fusion} = \xi * SourceStrength * E_{fusion} * Q \tag{29}$$

The source strength is the number of neutrons generated per second in the first wall. The Normalization factor is also used to obtain the flux level for the neutron flux spectra calculation and radiation damage calculations. PERCOSET multiplies the flux in each group and in each region by the normalization factor to obtain the actual flux levels in the reactor.

PERCOSET uses the power profile generated and rewrites the t-depl input file according to the new power level at the specific time step. Since the power is written in MW/MTHM (megawatts per metric ton heavy metal) PERCOSET has to scale the power level based off of the amount of HM in the region. It does this by dividing each region by the mass of HM in that region (volume of region * density of HM in region). After the depletion step is complete PERCOSET writes new cross section processing and depletion files with updated number densities after the depletion step.

After the new files are written PERCOSET determines whether the fuel needs to be shuffled or not. If the residence time of the fuel has been reached, PERCOSET shuffles the fuel according to the shuffling pattern being employed in that calculation. The calculation then can be started over if the cycle has yet to reach equilibrium, or if the cycle is in equilibrium the results can be analyzed. If the fuel has not reached the prescribed irradiation time the fuel is not shuffled and the calculation starts over at the pincell level and repeats itself until the irradiation time is reached.

PERCOSET is capable of doing irradiations in any time interval. For this paper a 250 day irradiation time was chosen. The 250 day interval was used to minimize the temporal changes in the power profile over the 750 day period.

Chapter 5 Fuel Cycle Scenarios

The primary objective of SABR is to obtain a deep burn of the transuranic isotopes. A deep burn is defined as greater than 90% burn up of the TRU fuel. There are in principle two possible ways in which achieving a deep burn of the transuranic isotopes can be accomplished: 1) a "once-through" cycle, with multibatch fuel shuffling but without fuel reprocessing and recycling; and 2) a "multi-batch cycle with repeated reprocessing and recycling of the TRU fuel remaining at the end of a multibatch burn cycle. The fuel residence time in the reactor is not limited by neutron balance criticality requirements in a sub-critical reactor, as it is in a critical reactor. However, the fuel residence time is limited by radiation damage to the clad and assembly structure and by allowable power peaking levels in both critical and sub-critical reactors. Since the radiation damage limit of 200 dpa adopted in this and many other studies limits the fuel burnup to well under 90%, a fuel cycle with reprocessing and recycling of fuel will be taken as the reference fuel cycle. However, once-through fuel cycles with a 200 dpa limit and with substantially higher limits that would enable achieving greater than 90% TRU burnup without reprocessing and recycling are also examined.

In meeting the objectives restrictions had to be placed on certain parameters in order to conform to SABR design assumptions, such as beginning of cycle (BOC) k_{eff} and end of cycle P_{fus} (fusion power). The limit set for BOC k_{eff} is 0.95 to provide a large margin to prompt criticality. The maximum amount of fusion power that can be obtained with the present neutron source design is 500 MW, which corresponds to a neutron strength of 1.77e20 n/s. This study explores the effects of shuffling pattern, cycle length, and the location and type of the reflector on the fuel cycle performance of SABR.

The fuel cycle performance of SABR will be characterized by 5 factors: (1) power profile, (2) overall transmutation rate, (3) tritium production, (4) decay heat load of the spent nuclear fuel, and (5) effective gain in repository space.

5.1 Power Profile

The power profile of the reactor is important because of the thermal properties and the cooling of the materials including the fuel in the reactor. If the power profile has steep gradients the local power density can vary considerably, within a single assembly; resulting in steep temperature gradients within each assembly. A problem that occurs when there are large temperature gradients is fuel bowing. Fuel bowing is an unwanted deformation of the fuel assembly. Thus minimizing the power peaking, equation 30, is critical to the overall performance of SABR.

$$PP = \frac{P_{\max}}{P_{average}} \tag{30}$$

P_{max} refers to the maximum local power density and $P_{average}$ is the average power density in SABR. Power peaking is determined by the fuel composition and the location of the fuel in the reactor. Methods to reduce power peaking include shuffling pattern, addition of a reflector, size **o**f reflector, and shortening the burn time.

5.2 Transmutation Rate

The overall transmutation rate in this study is defined as the Fissions of Initial Metal Atom (FIMA). FIMA is calculated with

$$FIMA = \frac{Initial - Final}{Initial} \tag{31}$$

where Initial is the initial amount of transuranics loaded at the beginning of cycle, and Final is the amount of transuranics that are in the fuel removed from the reactor at end of cycle. The higher the FIMA level for the reactor the greater overall transmutation rate.

5.3 Tritium Production

Tritium production is necessary in SABR to fuel the D-T fusion neutron source. Tritium is produced in the breeding blankets throughout the cycle. Enough tritium must be produced in the blankets accounting for decay for the fusion neutron source to operate. In principle, a tritium

breeding ratio (ratio of tritium production rate per fusion event) of TBR = 1.0 is sufficients. However, taking into account tritium decay and loss, TBR = 1.1 is a practical design objective.

5.4 Heat load

Lowering the long term heat load of the exiting fuel is a key goal in the evaluation of SABR's performance. Currently the amount of SNF that can be stored in Yucca Mountain is limited by the wall to wall drift temperatures as illustrated by figure 2 in the introduction. In order to reduce the required amount of repository space SABR must lower the integral heat production of the SNF that is to be stored at Yucca Mountain.

In this study the approach taken is a two step approach, first the fuel is burned in SABR lowering the amount of actinides that must be stored, and secondly the fission products are either separated out from the spent fuel and stored in a separate location because they produce a lot of heat, but decay away much more quickly than the actinides or the repository can be vented for the first couple hundred years to remove the large amount of initial decay heat produced by the fission products. Therefore in this study the heat load of the fission products are neglected because they do not have a significant contribution to the long term heat load (greater than 1000 years). For a once through cycle, this approach will maximize the reduction in required repository space necessary. In a reprocessing cycle the only waste product that needs to be stored are the fission products plus the contamination of the fission product stream by transuranics (1%) because the transuranics are being continuously recycled.

5.5 Shuffling Patterns

The length of the fuel cycle is determined by the residence time of fuel in the reactor, which is limited by radiation damage to the clad and other structural materials. A damage limit of 200 dpa is assumed for this purpose. For operation at 3000 MW_{th}, previous studies on SABR show the damage limit of 200 dpa is exceeded at 3080 days[26] corresponding to a fast fluence level of 5.26E23 n/cm^2; so 3000 effective full power days was chosen as the residence time for the fuel. Setting the residence time at 3000 days and choosing a 4 batch fuel cycle, chosen to correspond to the number of fuel rings in the core, led to a cycle length of 750 days.

This study goes through multiple scenarios to illustrate the effect of various fuel cycle choices on fuel cycle performance for SABR. The study started with analyzing two shuffling

patterns and a 750 day cycle time for a once-through non-recycling fuel cycle. The two shuffling patterns were an in-to-out pattern and an out-to-in pattern.

5.5.1 The Out-to-In shuffling pattern

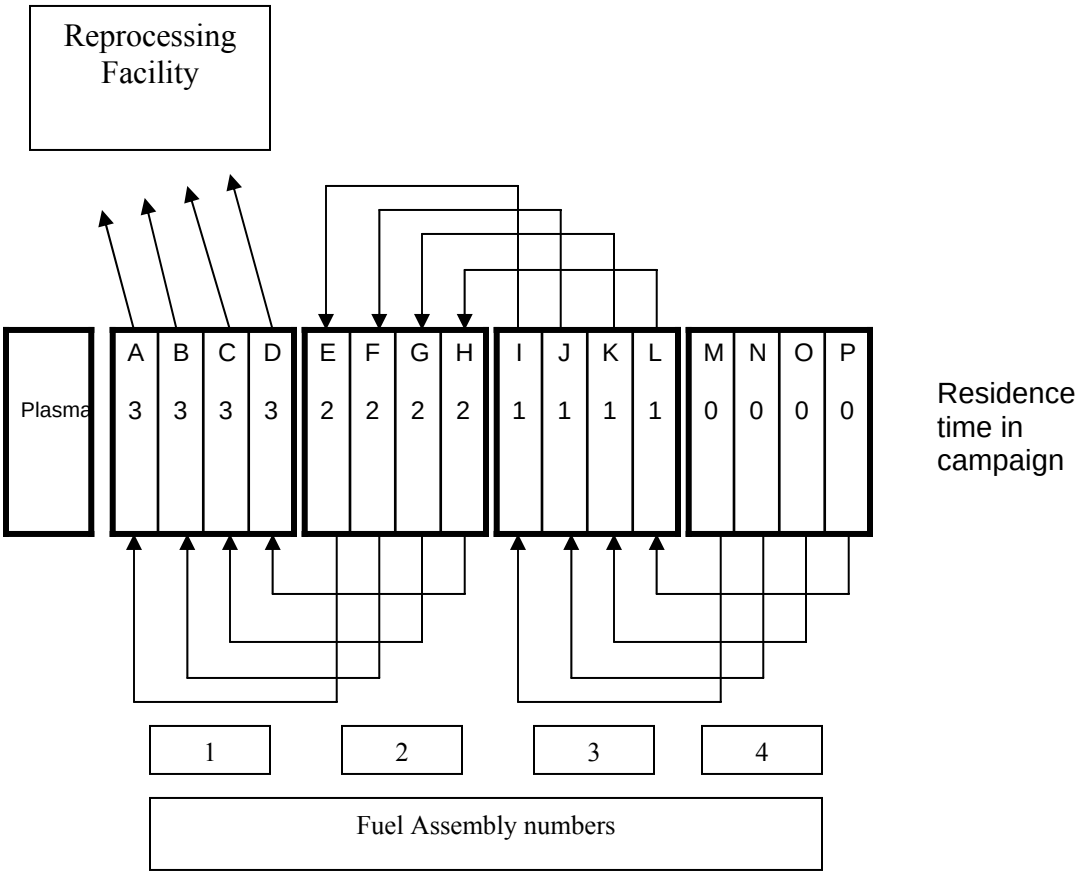

Figure 15: The Out-to-In shuffling pattern beginning of cycle

In the out-to-in scenario fresh fuel is loaded into regions M, N, O, and P (the outermost fuel assembly). After the fuel is burned for the set cycle time the fuel is shuffled one assembly inward. The fuel in assembly 4 moves to assembly 3, assembly 3 to assembly 2, and assembly 2 to assembly 1. All of the fuel in a fuel assembly is, of course, shuffled at the same time; the four regions in each assembly indicated in Fig. 15 are computational regions for the burnup analysis. The fuel that is removed from the innermost assembly one goes to either a reprocessing facility or geological disposal (although we are not proposing that fuel be burned in a 'once-through' cycle

and sent to a repository, we evaluate the effects of doing so for the purpose of illustration). Fresh fuel is inserted into assembly 4. Regions A-P represent the 16 different depletion regions in the calculational model. The depletion regions are shuffled on a per assembly basis such that region P is moved to region L, O to K, N to J, M to I, etc. The numbers in figure 15 represent the number of cycles the fuel has been in the reactor at beginning of cycle (BOC): 0 is fresh fuel, 1 is once burned, 2 is twice burned and 3 is three times burned. This results in the most reactive fuel being on the outboard side and the least reactive fuel being closest to the plasma neutron source. Reactivity is defined as:

$$\rho = \frac{k_\infty - 1}{k_\infty} \tag{31}$$

Furthermore, as a result of the discretization, the fuel in each assembly remains in the same assembly location, for instance the fuel in region P of assembly 4 is moved to region L of assembly 3.

5.5.2 In-to-Out Shuffling pattern

The in-to-out cycle shuffling pattern, shown in figure 16, is the exact opposite of the out-to-in pattern described in detail above; fresh fuel is loaded closest to the plasma and the fuel travels outward such that the outboard side of the core has the least reactive fuel at the end of cycle. This fuel is sent to the recycling facility.

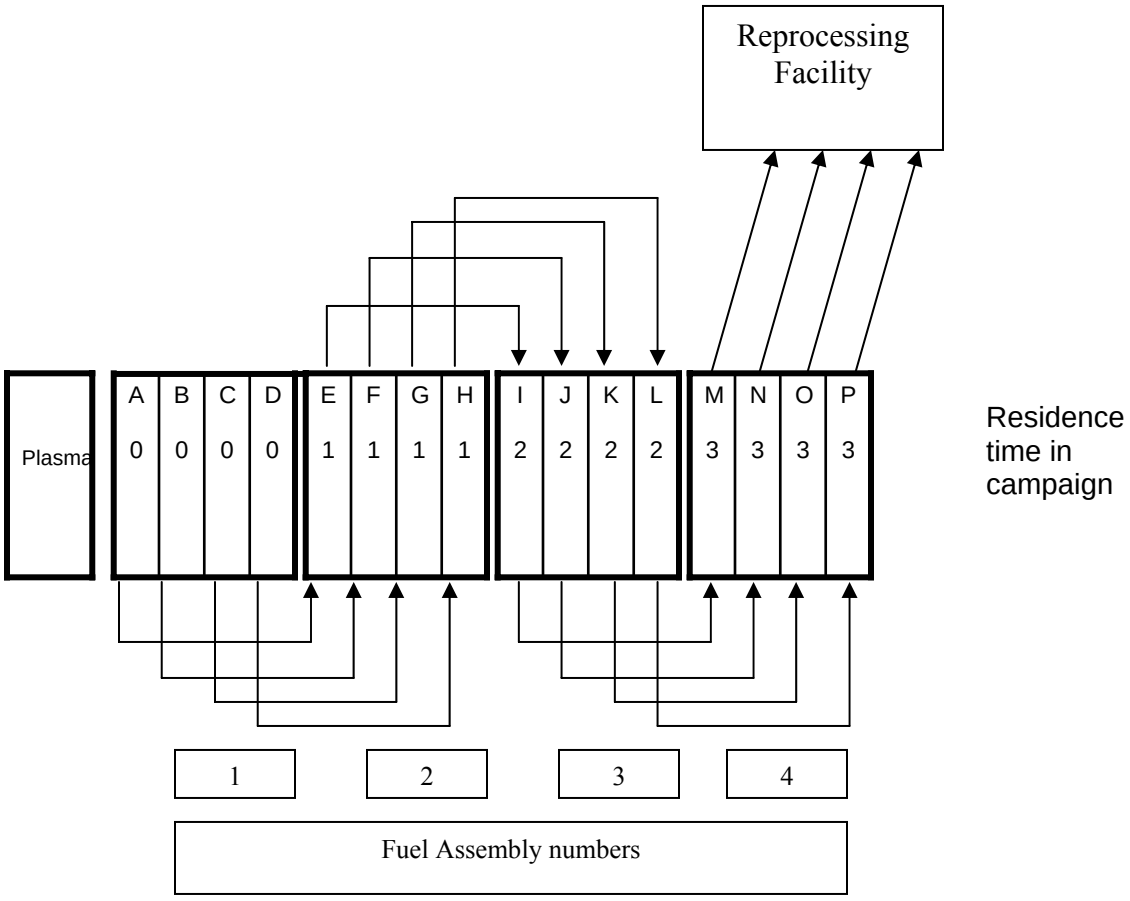

Figure 16: The in-to-out cycle shuffling pattern beginning of cycle.

Table 6 gives a list of the scenarios studied:

Table 6: Summary of fuel cycle scenarios

Scenario A	Out-to-In Shuffling pattern 4 750 day burn cycles no reprocessing 24% FIMA to Repository
Scenario B	In-to-Out Shuffling pattern 4 750 day burn cycles no reprocessing 24% FIMA to Repository
Scenario C	Out-to-In shuffling pattern 4 750 day burn cycles no reprocessing new reflector-blanket configuration 24% FIMA to Repository
Scenario D	Out-to-In shuffling pattern 4 3000 day burn cycles no reprocessing new reflector-blanket configuration 90% FIMA to Repository
Scenario E	Out-to-In shuffling pattern 4 750 day burn cycle reprocessing new reflector-blanket configuration only FP and reprocessing losses to the repository

In scenarios C, D, and E the lithium breeding blanket directly outside the core and the stainless steel reflector are interchanged and a thin graphite reflector is added. This was done to flatten the power profile in the core. The new core configuration at the outboard of the fission core is depicted in figure 17:

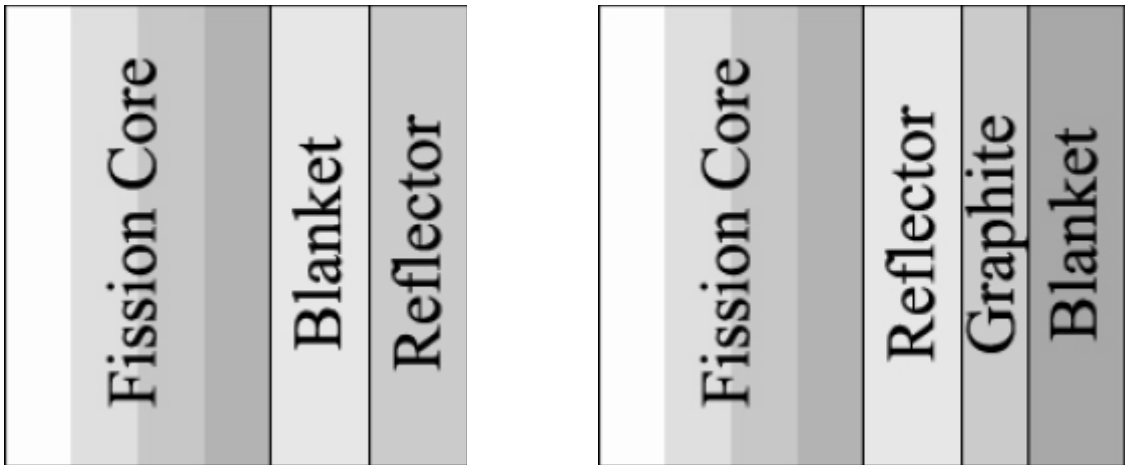

Original Configuration New Blanket Reflector Configuration

Figure 17: Changes in the reactor model to reduce power peaking

Scenario D is a study to investigate how long it would take to reach 90% burn up in one pass through the reactor if new materials were available with greater radiation damage limits. A fuel residence time of 12000 days would require radiation damage limits of greater than 200 dpa for the fuel assembly material and the cladding material.

Finally Scenario E explores achieving greater than 90% burnup with the present 200 dpa radiation damage limit by reprocessing the spent fuel from SABR after the 3000 day cycle time to recover the remaining TRU to be re-fabricated into fuel and recycled New material (TRU) is added to the reprocessed TRU in the fabrication process. The same 4 batch out-to-in fuel cycle is repeated with the reprocessed fuel, etc.

Chapter 6: Transmutation Performance

6.1 Scenarios A and B: Out-to-In and In-to-Out shuffling patterns with a 750 day burn cycle no reprocessing or recycling 24% FIMA to repository

A comparison of the in-to-out and out-to-in scenarios was done to determine which shuffling pattern would be used in the rest of the scenarios. Table 7 summarizes the results of this cycle.

Table 7: Major Fuel Cycle Parameters

		Fuel Cycle	
Parameter	Units	Out to in	In to out
Thermal Power	MW	3000	3000
Cycles per Residence Time		4	4
Burn Cycle Length Time	Days	750	750
4 Batch Residence Time	Years	8.21 y	8.21 y
BOC keff		0.902	0.914
EOC keff		0.848	0.859
BOC Pfus	MW	180	164
EOC Pfus	MW	240	228
TRU BOC Loading	MT	36	36
Power Density	KW/kg	83.3	83.3
Power Peaking BOC		1.25	1.76
Power Peaking EOC		1.56	1.81
TRU Burned per Residence	%	23.1%	23.02%
TRU Burned per Year	MT/FPY	1.02	1.01
TRU Burned per Residence	MT	8.32	8.29
SNF Disposed per Year	MT/FPY	102	101
LWR Support Ratio		4	4
Average Core Flux Across Cycle	n/cm^2-s	1.33E15	1.02E15
Average Fast (>0.1 MeV) Flux	n/cm^2-s	8.60E14	6.20E14
Fluence per Residence Time	n/cm^2	3.45E23	2.64E23
Fast Fluence	n/cm^2	2.23E23	1.36E23
Hardness of Spectrum	%	64.7%	51.7%
Heat Load After 100,000 years	W/kg TRU Initial	.112	.118
Heat Load after 100,000 years SABR Input	W/kg TRU Initial	.127	.127
Integral Heat Load	W/kg TRU Initial	48834	48015
Integral Heat Load (SABR Input)	W/kg TRU Initial	88705	88705
Reduction in Required Repository Space		1.81	1.85

Many of the terms used in the output tables require greater explanation. The "TRU Burned per Residence" refers to the amount of TRU burned per batch per residence time. It is calculated by using the FIMA formula of equation 31. The "SNF Disposal Rate" is the mass of SNF whose TRU content is burned in one FPY (full power year) in SABR. The TRU content in the SNF is approximately 1 % of the SNF[33] and approximately 1.02 MT TRU are burned per FPY the SNF rate is about 102 MT/FPY.

The "LWR Support Ratio" is defined as the amount of TRU destroyed by SABR to the amount of TRU produced by a 1000 MWe LWR. On average a 1000 MWe LWR produces 250 kg TRU per year[35] as compared to the 1.02 MT TRU per year burned by SABR.

The hardness of the spectrum is calculated via:

$$R = \frac{\int_{100Kev}^{\infty} \phi(E)de}{\int_{0}^{\infty} \phi(E)de} \tag{33}$$

This ratio of the flux greater than 100 keV to the total flux results in a harder spectrum for the Out-to-In cycle (64.7% fast flux) than the In-to-Out cycle (51.7% fast flux). The total fast flux for the In-to-Out cycle is about 60 percent lower than the Out-to-In cycle which would allow for operation of 1.6 times longer without exceeding radiation damage limits.

The heat load numbers after 100,000 years show a small difference at 24% FIMA. The integral heat is reduced by almost a factor of two from the initial TRU input into SABR. This results in a reduction in required repository space by a factor of 1.8 for both shuffling patterns.

6.1.1 Power Distribution

The first comparison that can be made is that of the power profiles. Figure 18 contains both the beginning of cycle (BOC) and end of cycle (EOC) power profile for each cycle.

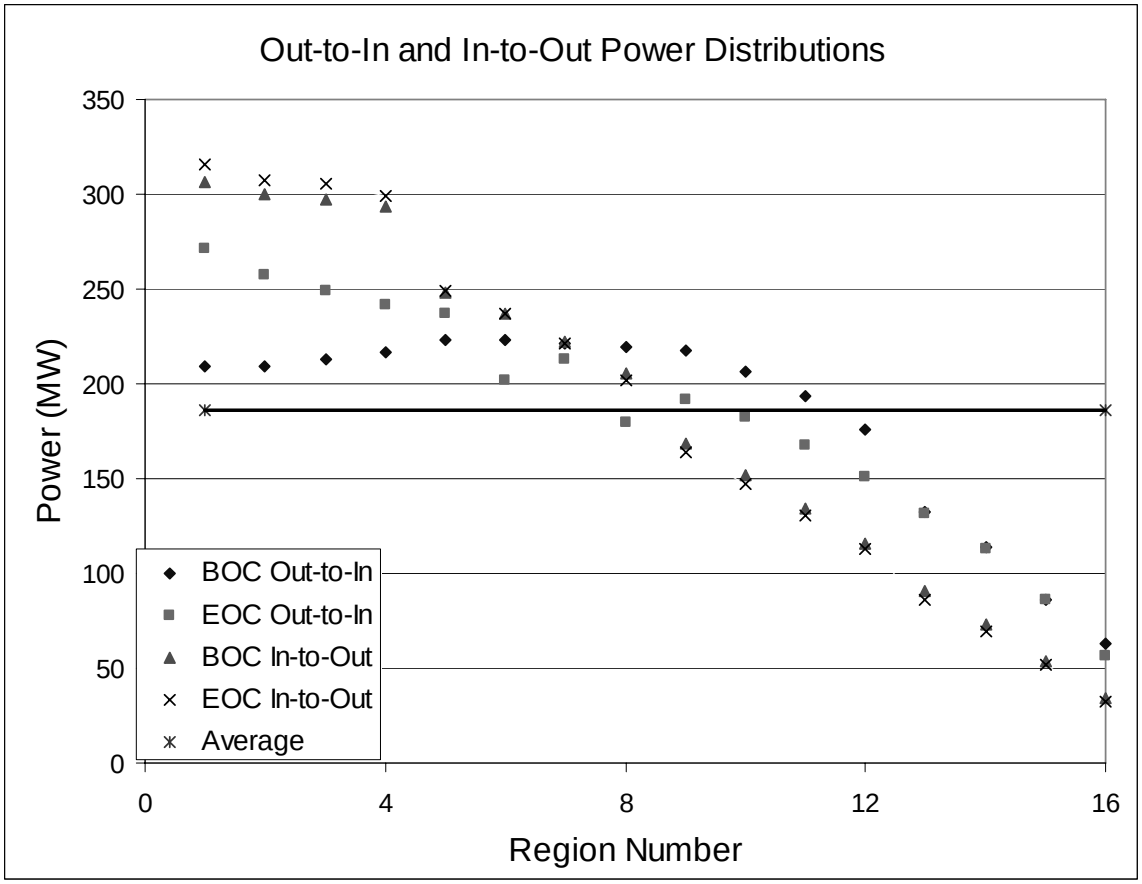

Figure 18: Power Distribution Comparison of the In-to-Out and the Out-to-In Cycle at both BOC and EOC

Both cycles have very large gradients in the power distribution especially at the end of cycle. The Out-to-In cycle seems to be slightly better in this situation than the In-to-Out. The maximum power peaking values for BOC and EOC for the Out-to-In are 1.25 and 1.56. For the In-to-Out cycle the BOC and EOC values for power peaking are 1.76 and 1.81. More detailed work can be done in trying to improve the power distribution. Rotating the fuel assemblies 180 degrees during the shuffling of the fuel could improve the power distribution. Also zoning the fuel concentrations within each assembly would result in a flatter power distribution. Both of these considerations are beyond the scope of this work.

6.1.2 Transmutation Rate

Another comparison that goes into effect as to which shuffling pattern resulted in a greater overall performance is that of TRU burned per residence. Since the goal of the study is to

transmute greater than 90% of the transuranics the greater amount of destruction per residence results in better performance. In both instances the reactor operates at 3000 MW_{th}, therefore the number of fissions in both shuffling patterns should be the same. The Out-to-In pattern resulted in a slightly greater percentage of burn up than the In-to-Out shown in table 8 at the beginning of this section.

6.1.3 Radiation Damage

The radiation damage must also be considered in choosing the shuffling pattern. Radiation damage is calculated based on the fast fluence (greater than 100 keV) seen by each component in the reactor. Fluence is defined as the time integrated scalar flux. If one shuffling pattern results in a significantly higher fast fluence than another shuffling patterns the length of that cycle decreases. As the cycle length decreases the net amount of transmutation decreases leading to a less efficient cycle. The limiting materials factor in SABR is the radiation damage to structural materials. Figures 19 and 20 show the neutron energy spectrum for both the In-to-Out and Out-to-In shuffling patterns.

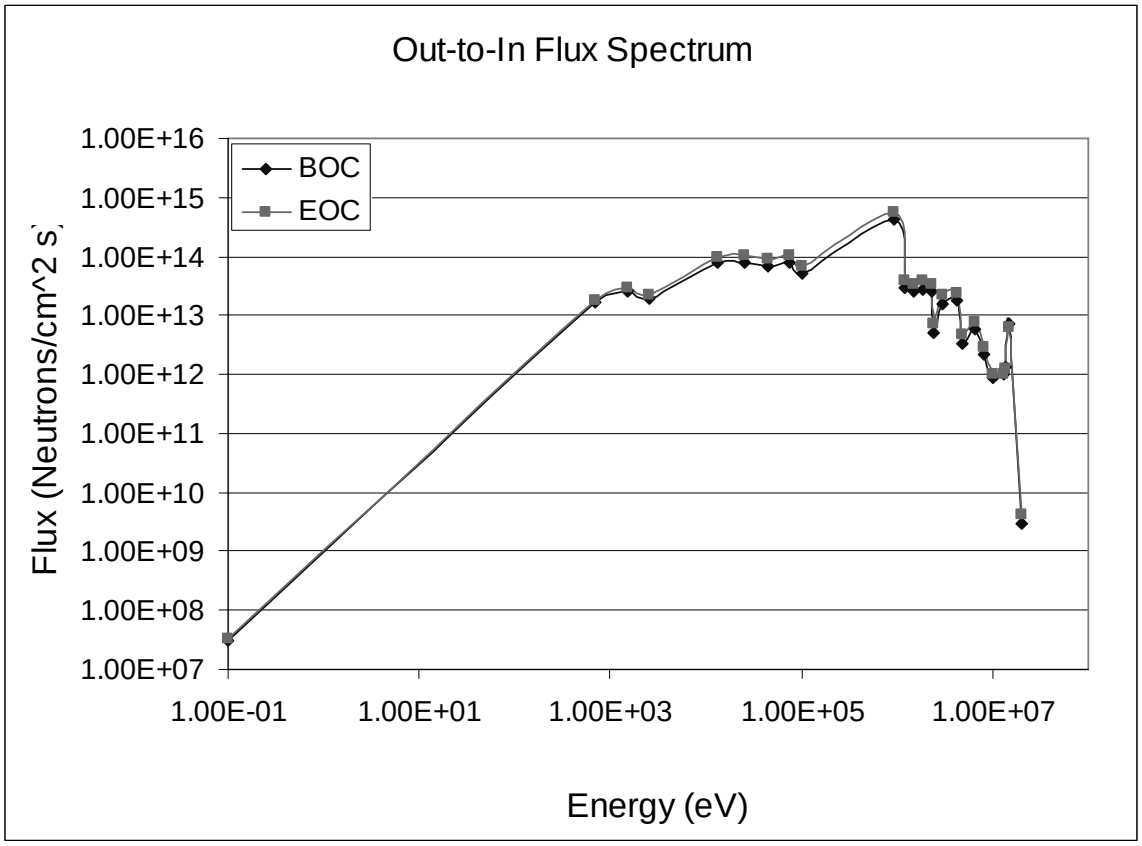

Figure 19: In-to-Out Neutron Spectrum averaged over the entire core at BOC and EOC

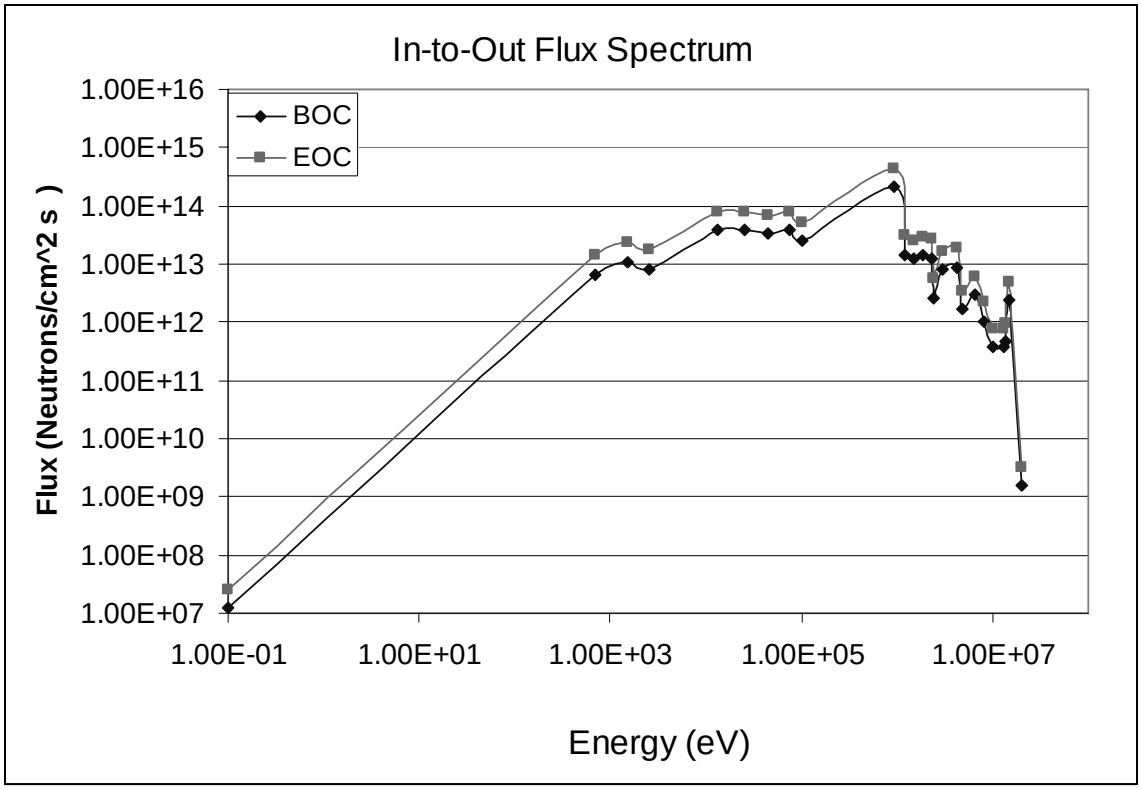

Figure 20: Out-to-In Neutron Spectrum averaged over the entire core at BOC and EOC

Both spectra peak in the energy group between 100keV and 920 keV with the majority of the flux contained between 1keV and 10 MeV. The fast fluence in each shuffling pattern is similar, 2.23E23 for Out-to-In as opposed to 1.36E23 for In-to-Out, and thus for the radiation damage criteria the cycles are equivalent.

6.1.4 Tritium Production

Tritium production needs to be considered in the determination of shuffling pattern. Table 8 shows the tritium production and destruction at the beginning of cycle and end of cycle and the tritium breeding ratio. The tritium destruction is based off of the fusion power level, the higher the fusion power the greater the destruction rate. The tritium production rate is determined by multiplying the neutron flux that reaches the breeding blanket with the (n,α) cross section of the lithium in the blanket. The specific equations as well as the calculation for tritium necessary at BOC can be found in section 4.5. For these two cycles it was found that SABR was tritium self sufficient.

Table 8: Tritium Production

	Out-to-In	In-to-Out
BOC Tritium Destruction	7.53e19 atoms/second	6.46e19 atoms/second
BOC Tritium Production	3.82e20 atoms/second	3.54e20 atoms/second
EOC Tritium Destruction	8.49e19 atoms/second	8.21e19 atoms/second
EOC Tritium Production	5.78e20 atoms/second	5.33e20 atoms/second
Tritium Necessary for BOC	6.88e21 atoms	6.00e21 atoms
Tritium at BOC	6.93e21 atoms	6.10e21 atoms

6.1.4 Heat Load to Repository

Finally a comparison of the heat load is done for each cycle and the effective gain in repository space. The cumulative amount of heat given off by the SNF is the quantity that governs the capacity of the geological repository. These criteria are all similar to each other because they all are a function of burnup, which is similar for both shuffling patterns. Figures 21 and 22 are comparisons of the decay heat in the fuel that is input into SABR and the in-to-out and out-to-in shuffling pattern.

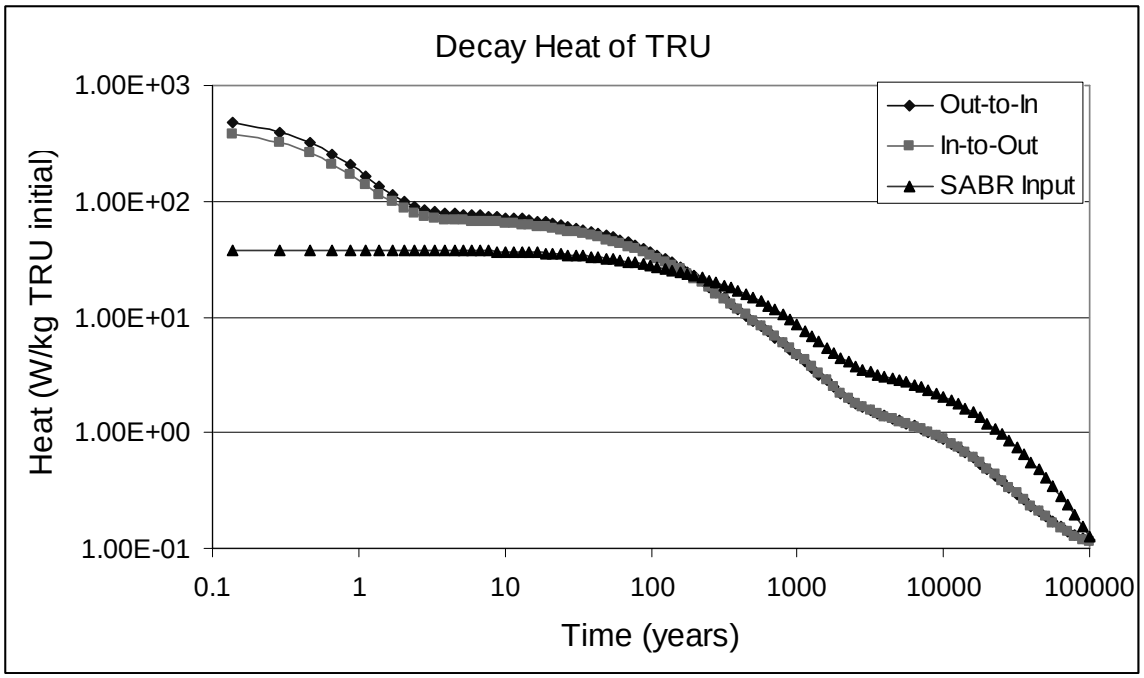

Figure 21: Decay heat production from TRU for Out-to-In cycle, In-to-Out cycle, and SABR Input fuel

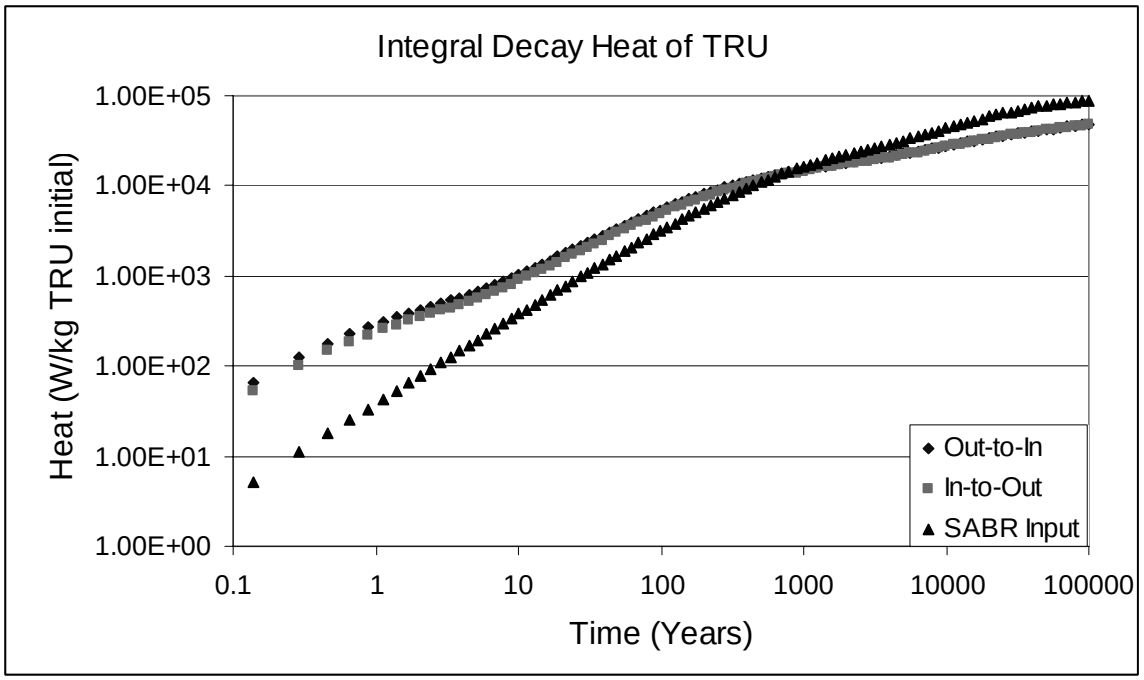

Figure 22: Integral Decay heat from TRU of the Out-to-In cycle, In-to-Out cycle, and SABR Input fuel

The increase in decay heat when burning approximately 23% of the transuranics is caused by neutron capture and the formation of higher actinides that have shorter half lives. Figure 23 shows the decay heat that is produced per isotope. Each curve represents the heat produced from a specific isotope and all of its progenies. For example the ^{242}Cm alpha decays to ^{238}Pu which then alpha decays to ^{234}U and the decay heat of the alpha decay of ^{238}Pu is included in the ^{242}Cm curve.

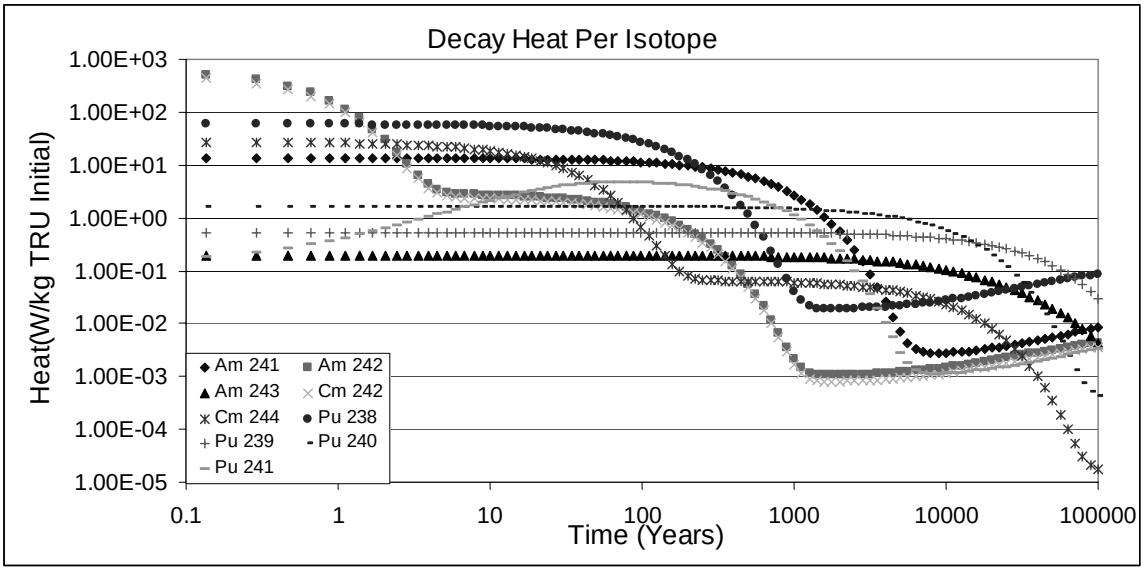

Figure 23: Decay heat per isotope in the Out-to-In fuel cycle

The largest limitation to what can be stored in deep geological storage (Yucca Mountain) is the cumulative amount of heat generated. As is shown in figures 21 and 22 a burn up of 23% initially would increase the decay heat and only slightly decrease the long-time cumulative decay heating if the 23% burned fuel from once-through cycle was actually put in a geological repository. This problem is caused by the increase in drift wall temperature at emplacement. The drift wall temperatures at enclosure would be lower for these cycles because the integral decay heat is lower after approximately 1000 years. The integral decay heat from the TRU in the out-to-in cycle is 48830 W/kg TRU input, the in-to-out cycle is 48020 W/kg TRU input, and the fuel input into SABR is 88705 W/kg TRU input. The integral decay heat would be reduced by approximately a factor of 2 for each scenario, which would reduce the required repository requirements for storing the spent fuel by a factor of 2. This probably would not be a big enough

reduction to justify the cost, and the results of such a fuel cycle are shown only for illustrative purposes.

6.1.5 Summary of Scenarios A and B

These scenarios indicate that a single pass burnup of greater than 90% is not possible with a batch residence time of 3000 days. The results also show that there is very little to gain using once through transmutation to a FIMA level of 24%. Ultimate disposal of this fuel is not an attractive option because it does not lower the overall heat load enough to reduce the amount of TRU to be stored in repository by a significant amount.

The major difference in the two shuffling patterns occurred in the power distribution and in the fast neutron fluence. It was shown that the Out-to-In cycle has a much flatter power distribution than the In-to-Out pattern. The higher fast neutron fluence in the out-to-in cycle results in a higher rate of damage accumulation. This higher rate of damage accumulation will result in a shorter maximum cycle time than the in-to-out cycle. The shorter cycle time is not an issue in this study because the radiation damage limit is exceeded after the 3000 day cycle time. The other comparison that showed a difference was that of the percent burn up or FIMA. The Out-to-In shuffling pattern resulted in a FIMA of 23.1% where the In-to-Out only had 23.02% FIMA. The In-to-Out pattern was superior in it used less fusion power but since both patterns are below the 500 MW that can be produced by the fusion source either cycle is an option. Thus the rest of the calculations are based on the Out-to-In cycle.

6.2 Scenario C: 750 day fuel cycle Out-to-In pattern new blanket reflector configuration

The goal of this scenario was to examine the effect of a SABR design change to reduce the amount of power peaking in the out-to-in scenario by switching the location of the breeding blanket and the reflector and incorporating a layer of graphite between the reflector and the breeding blanket to try and reflect more neutrons. Table 9 summarizes the results of this scenario.

Table 9: Fuel Cycle Parameters Scenario C

		Fuel Cycle	
		Scenario C	Scenario A
Parameter	Units	Values	
Thermal Power	MW	3000	3000
Cycles per Residence Time		4	4
Burn Cycle Length Time	Days	750	750
4 Batch Residence Time	Years	8.21 y	8.21 y
BOC keff		0.926	0.902
EOC keff		0.876	0.848
BOC Pfus	MW	151	180
EOC Pfus	MW	208	240
TRU BOC Loading	MT	36	36
Power Density	KW/kg	83.3	83.3
Power Peaking BOC		1.12	1.25
Power Peaking EOC		1.31	1.56
TRU Burned per Residence	%	23.6%	23.1%
TRU Burned per Year	MT/FPY	1.03	1.02
TRU Burned per Residence	MT	8.4996	8.32
SNF Disposed per Year	MT/FPY	103	102
LWR Support Ratio		4	4
Average Core Flux Across Cycle	n/cm^2-s	5.46E15	1.33E15
Average Fast (>0.1 MeV) Flux	n/cm^2-s	3.47E15	8.60E14
Fluence per Residence Time	n/cm^2	1.42E24	3.45E23
Fast Fluence per residence Time	n/cm^2	9.03E23	2.23E23
Hardness of Spectrum	%	63.6%	64.7%
Heat Load after 100,000 years	W/Kg TRU Initial	.151	.112
Integral Heat Load	W/Kg TRU Initial	46868	48834
Reduction in Required Repository Spac	Factor	1.89	1.81

The BOC and EOC k_{eff} in this scenario were higher than in the previous scenarios, 0.926 versus 0.902 for BOC and 0.876 versus 0.848 for EOC, this is due to more reflection caused by the new blanket reflector configuration. The power peaking was reduced by 10 percent at the beginning of cycle and by 16 percent at the end of cycle with the new reflector design. Even though the ratio of the fast flux to total flux is lower in this scenario resulting in a softer spectrum the total flux is higher. The increase in the total flux is caused by the softer spectrum and not as many threshold fission reactions are occurring because there is less fast flux. This higher flux results in more radiation damage and decreases the lifetime of this cycle by a factor of 4.

6.2.1 Power Distribution

As stated earlier the goal of this scenario was to try and flatten the power distribution by introducing a new reflector blanket configuration. Figure 24 below shows that the new reflector blanket configuration flattens the overall power profile and reduces the amount of power peaking in the reactor.

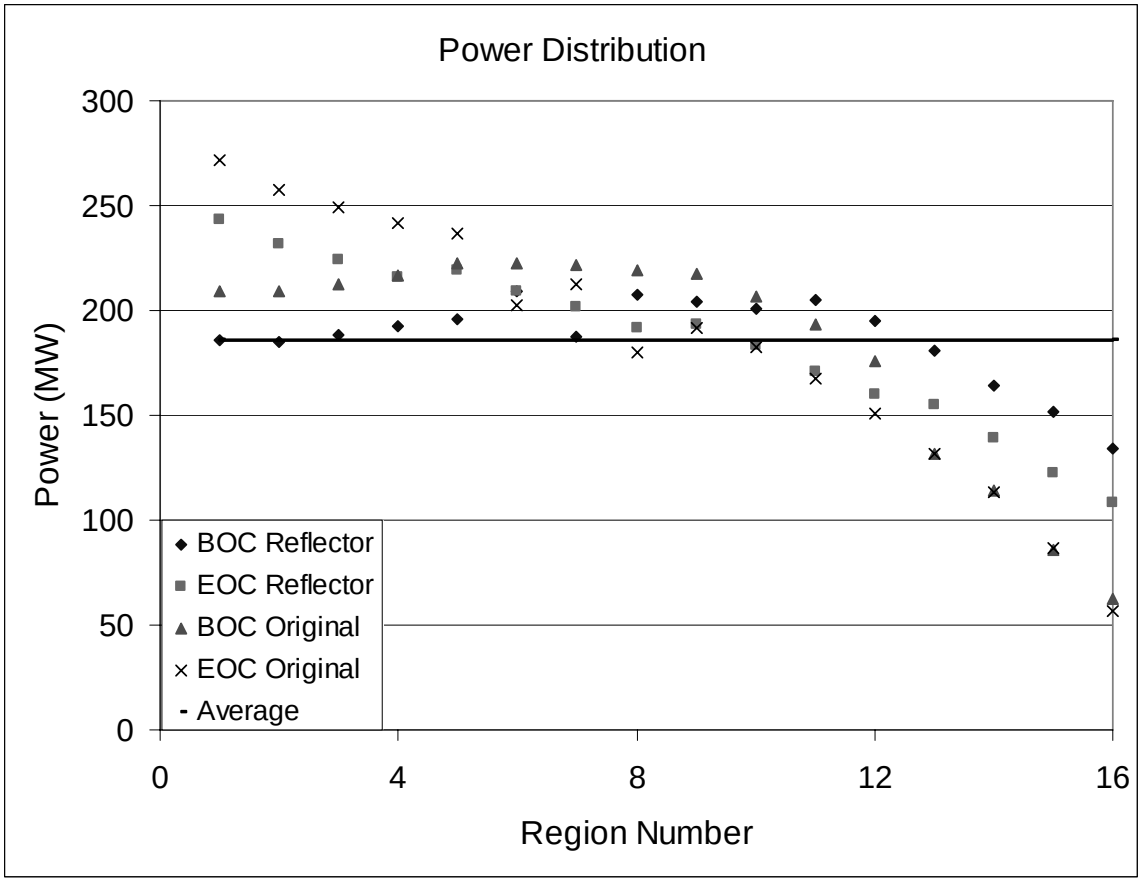

Figure 24: Power distribution comparison of the new blanket reflector configuration with the original blanket reflector at BOC and EOC

The flatter power distribution in this cycle is due to reflection of neutrons back into the system by the new reflector configuration. The increased reflection results in a softer spectrum in the outermost regions of the core. The softer spectrum and the increase in the number of neutrons in the outer regions increases the number of fission reactions that occur. The increase in the number of fission reactions occurring increases the power generated in the outer regions.

6.2.2 Radiation Damage

The resulting neutron energy spectrum is similar to the Out-to-In cycle studied in scenario A except it is a softer spectrum. The softer spectrum is a result of less fusion power necessary for the cycle and the new reflector configuration moderating the reflected neutrons to lower energies. Figure 25 shows the flux spectrum for this scenario:

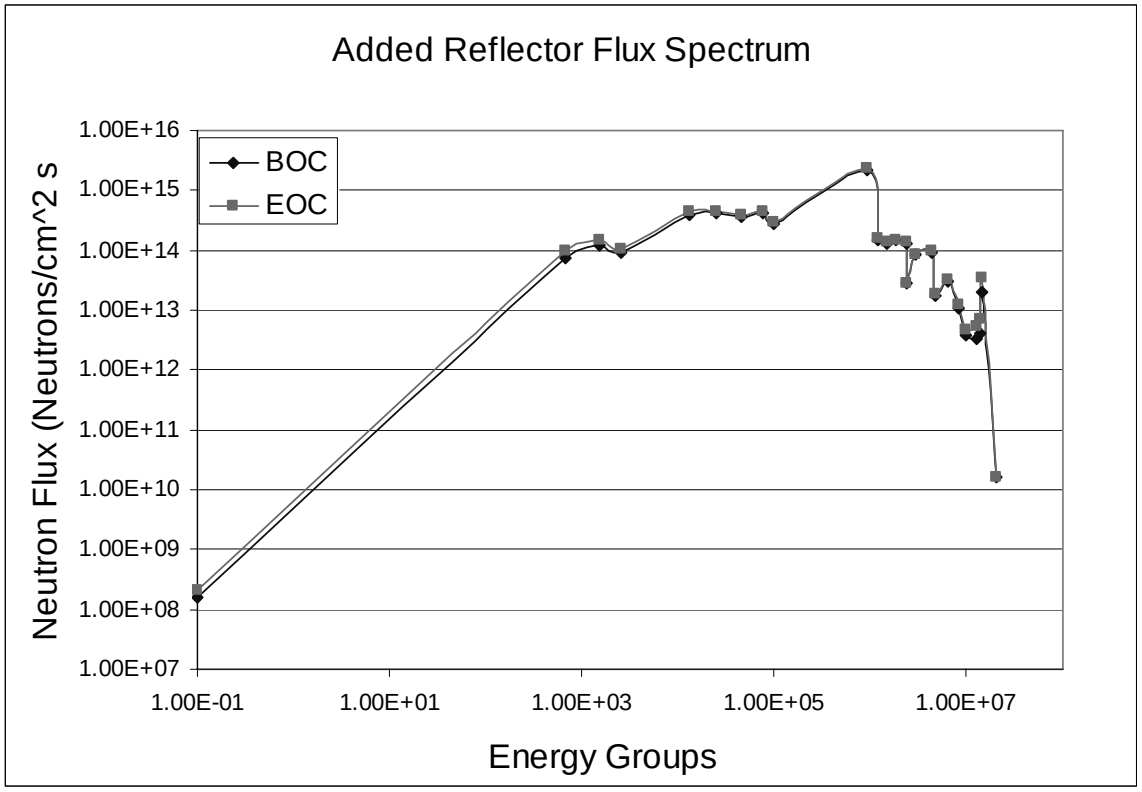

Figure 25: Neutron Flux Spectrum averaged over the core for Scenario C at BOC and EOC

6.2.3 Tritium Production

Tritium production, destruction and self sufficiency shown in Table 10 below: The tritium produced at BOC is within 1% of the conservative estimate of that needed for tritium self-sufficiency, so the design could certainly be modified to achieve tritium self-sufficiency. This table was produced in the same manner as table 8 in section 6.1.3.

Table 10: Tritium Production

BOC Tritium Destruction	5.36e19 atoms/second
BOC Tritium Production	2.34e20 atoms/second
EOC Tritium Destruction	7.38e19 atoms/second
EOC Tritium Production	3.76e20 atoms/second
Tritium Necessary for BOC	5.04216e21 atoms
Tritium at BOC	4.99e21 atoms

6.2.4 Heat Production

The gamma heat load and the activity per unit kg TRU exiting SABR was lower for the reflector cycle. The figure of the decay heat load and integral decay heat is shown in figures 26 and 27 below:

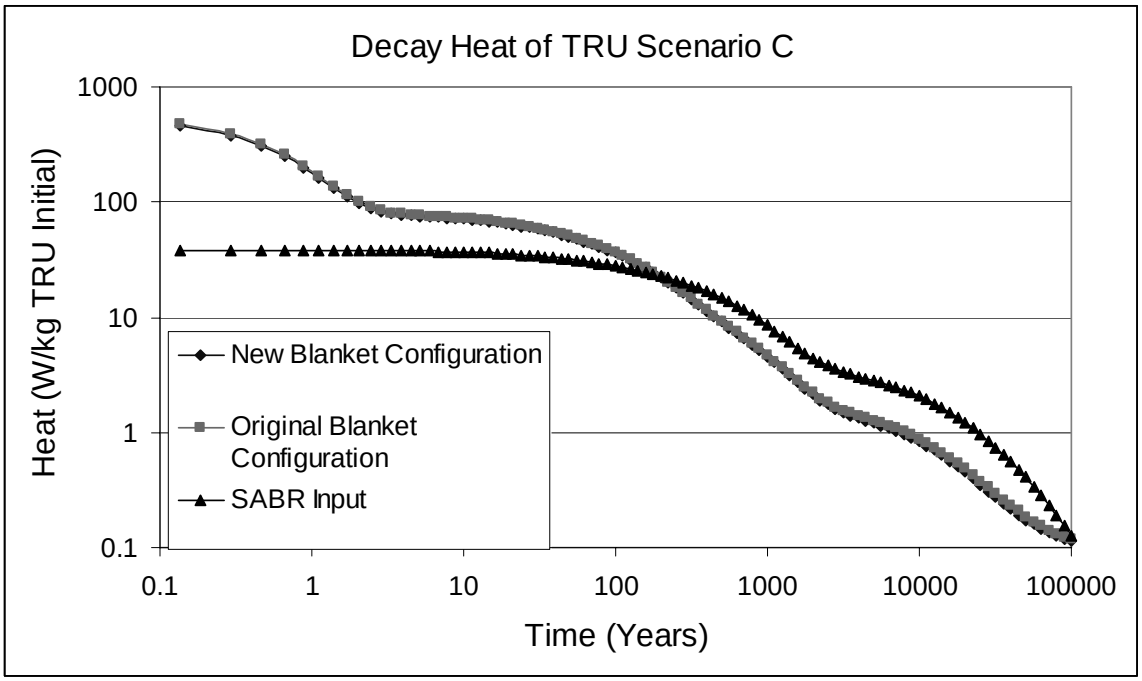

Figure 26: Decay Heat for New Blanket Configuration, Original Blanket Configuration, and SABR Input Fuel

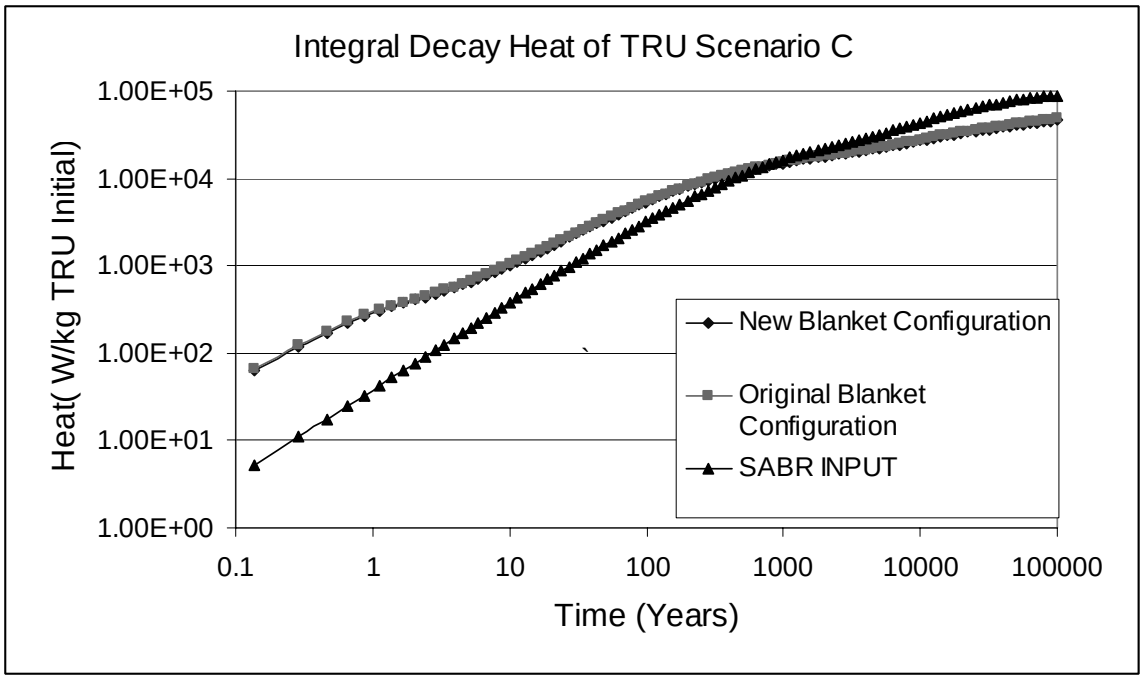

Figure 27: Integral Decay Heat for New Blanket Configuration, Original Blanket Configuration, and SABR Input Fuel

These figures show that the integral heat for the new reflector blanket configuration is similar to the original blanket configuration, 46868 W/kg are produced in the new configuration versus 48834 W/kg in the original configuration this results in a reduction in required repository space of 1.89 for the new configuration as opposed to 1.81 for the original configuration.

6.2.5 Summary of Scenario C

This scenario shows that similar results are obtained in the transmutation and heat load to the repository. The goal of flattening the power profile was obtained while still maintaining tritium self sufficiency and a low enough radiation damage to operate for a 3000 day residence time. Therefore the new reflector blanket configuration is adopted and the design of SABR was changed for the rest of this work.

6.3 Scenario D: 3000 day burn cycle time (12000 day residence)

The purpose of scenario D was to extend the fuel residence time to achieve greater than 90% burnup in a once-through cycle without fuel reprocessing and recycling, assuming that a

structural material that could survive the corresponding level of radiation damage were developed. Table 11 summarizes the results of this fuel cycle.

Table 11: Scenario D fuel cycle results

		Fuel Cycle	
		Scenario D	Scenario A
Parameter	Units	Values	
Thermal Power	MW	3000	3000
Cycles per Residence Time		4	4
Burn Cycle Length Time	Days	3000	750
4 Batch Residence Time	Years	24.65 y	8.21 y
BOC keff		0.677	0.902
EOC keff		0.476	0.848
BOC Pfus	MW	433	180
EOC Pfus	MW	663	240
TRU BOC Loading	MT	36	36
Power Density	KW/kg	83.3	83.3
Power Peaking BOC		4.80	1.25
Power Peaking EOC		4.54	1.56
TRU Burned per Residence	%	91.2%	23.1%
TRU Burned per Year	MT/FPY	0.84	1.02
TRU Burned per Residence	MT	20.736	8.32
SNF Disposed per Year	MT/FPY	84	102
LWR Support Ratio		4	4
Average Core Flux Across Cycle	n/cm^2-s	9.65E15	1.33E15
Average Fast (>0.1 MeV) Flux	n/cm^2-s	7.14E15	8.60E14
Fluence per Residence Time	n/cm^2	1.00E25	3.45E23
Fast Fluence per Residence Time	n/cm^2	7.40E24	2.23E23
Hardness of Spectrum	%	74.0%	64.7%
Heat Load after 100,000	W/kg TRU Initial	.104	.112
Integral Heat Load	W/kg TRU Initial	6834	48834
Reduction in Required Repository Space	Factor	13	1.81

In this scenario the BOC k_{eff} is much lower in this fuel cycle (0.677 versus 0.926) because the equilibrium cycle has fuel that has been irradiated for 3000,6000, and 9000 days as opposed to the 750,1500,2250 days for the 3000 day fuel cycle. The BOC k_{eff} of 0.677 results in a fusion power of 433 MW, which is still below the 500 MW that can be produced by the SABR fusion neutron source. The EOC k_{eff} was 0.476 resulting in a fusion power of 633 MW which would require slight extensions of the SABR neutron source design. The minimum k_{eff} which SABR can be operated at is 0.62; below this value the neutron source is not strong enough to sustain 3000 MW_{th}.

The longer residence time results in a larger reduction in the integral heat load. The greatly reduced integral heat load reduces the required repository space by a factor of 13.

6.3.1 Power Distribution

The power distribution for this cycle is shown in figure 28 below.

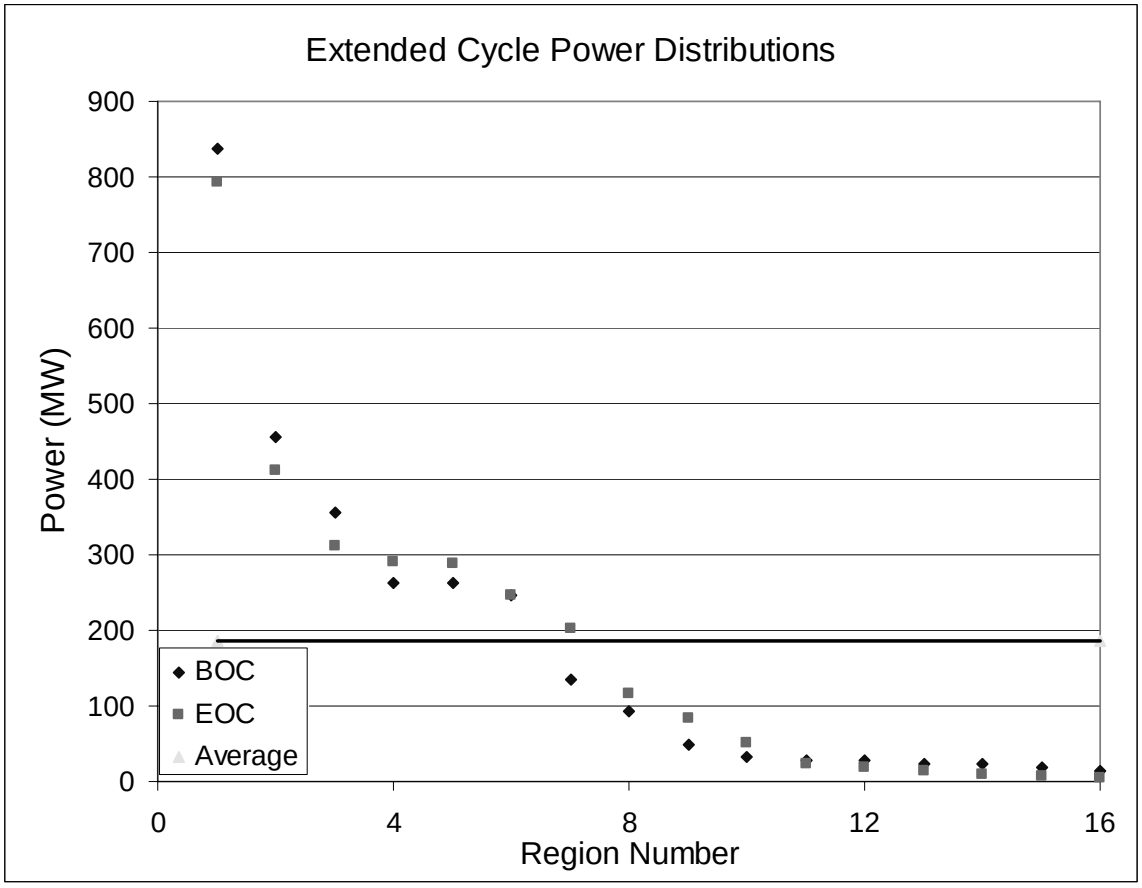

Figure 28: Extended Cycle Power Distribution at BOC and EOC

The power distribution in this scenario can be explained by diffusion theory. Assume a subcritical infinite half slab with a planar neutron source on the left boundary. The diffusion equations below were solved and Figure 29 shows the solution for the flux shape for each case. A calculation was done and k_{inf} of the first assembly was calculated as 0.34.

$$-\nabla D\nabla\Psi + \Sigma_a\Psi = \nu\Sigma_f\Psi + S \tag{33}$$

Where D is the diffusion coefficient and S is the source term. The source term is described as:

$$S = S_0 * \delta \tag{34}$$

Rearranging the terms in equation 33

$$-\nabla D\nabla\Psi + (\Sigma_a - \nu\Sigma_f)\Psi = S \tag{35}$$

$$\nabla D\nabla\Psi + (\nu\Sigma_f - \Sigma_a)\Psi = -S \tag{36}$$

Assuming that the diffusion coefficient is constant in space equation 36 can be transformed into:

$$D\nabla^2\Psi + (\nu\Sigma_f - \Sigma_a)\Psi = -S \tag{37}$$

$$\nabla^2\Psi + \frac{(\nu\Sigma_f - \Sigma_a)\Psi}{D} = -\frac{S}{D} \tag{38}$$

$$\nabla^2\Psi + B_m^2\Psi = -\frac{S}{D} \tag{39}$$

If:

$$B_m^2 < 0,\ \nu\textstyle\sum_f < \sum_a$$
$$B_m^2 = 0,\ \nu\textstyle\sum_f = \sum_a$$
$$B_m^2 > 0,\ \nu\textstyle\sum_f > \sum_a$$

the three solutions in Figure 29 are found.

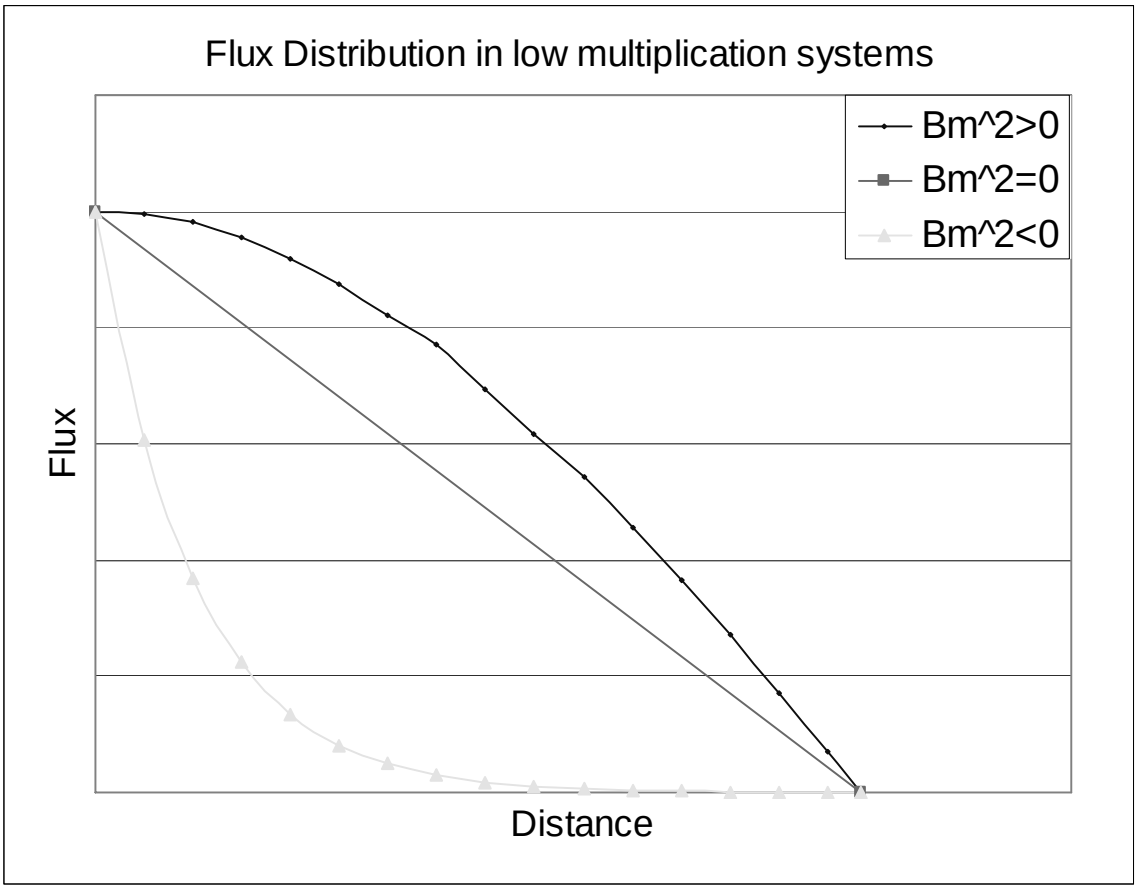

Figure 29: Diffusion Theory flux distribution for subcritical infinite slab

6.3.2 Radiation Damage

The flux spectrum in this scenario is much harder than the rest of the scenarios which is caused by the much larger fusion neutron source. Since the fuel has a lower multiplication constant there are more fusion neutrons entering the core, this larger fraction of 14 MeV neutrons in the core is what causes the harder spectrum that can be seen in figure 30.

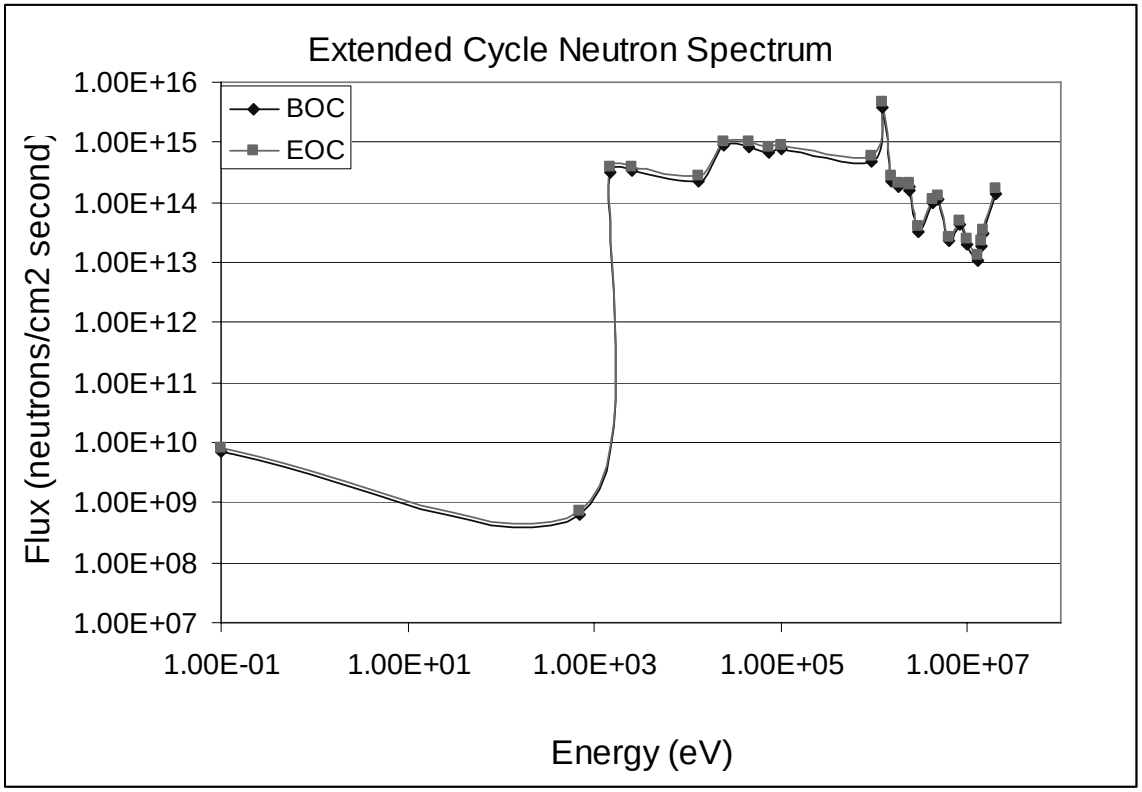

Figure 30: Neutron Energy Spectrum Averaged over the Core at BOC and EOC

6.3.3 Tritium Production

In this cycle it is necessary to produce more tritium throughout the cycle due to the higher fusion power. The amount of tritium that was produced using the method that has been described in both sections 4.5 and 6.1.3. The required amount of tritium produced for this cycle is just short of the amount necessary for self sufficiency. This is not a problem because the assumptions made in the calculations of the production of tritium are conservative. Also there is room to make the blanket thicker which would increase the amount of tritium produced.

Table 12: Tritium Production

BOC Tritium Destruction	1.54e20 atoms/second
BOC Tritium Production	1.86e20 atoms/second
EOC Tritium Destruction	2.35e20 atoms/second
EOC Tritium Production	1.38e21 atoms/second
Tritium Necessary for BOC	1.47e22 atoms
Tritium at BOC	1.45e22 atoms

6.3.4 Heat Load to the repository

The heat load per kg TRU in this scenario is much lower in the other scenarios. The overall heat load and activity is also much lower in this scenario because we have transmuted 91.2% of the minor actinides as compared to 23% in the other cycles. Since the fission products have been separated out for individual storage and the only components of the fuel being analyzed are the actinides the higher burn up is what causes the lower heat load.

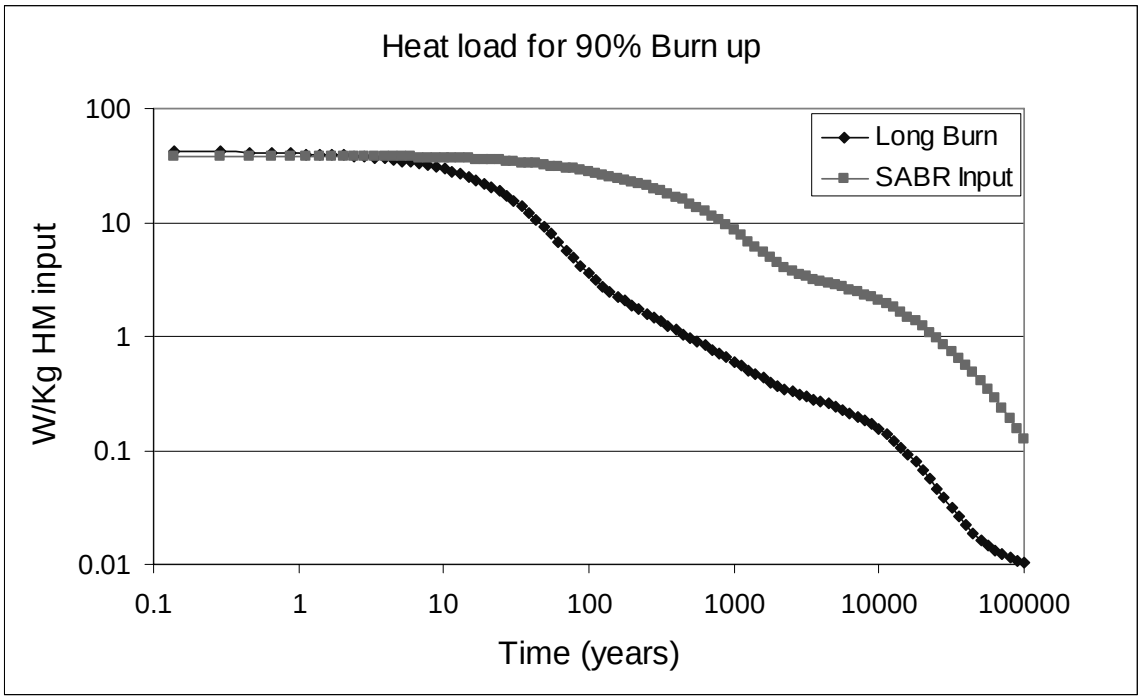

Figure 31: Heat Load at 90% Burn Up for the Extended Burn Cycle

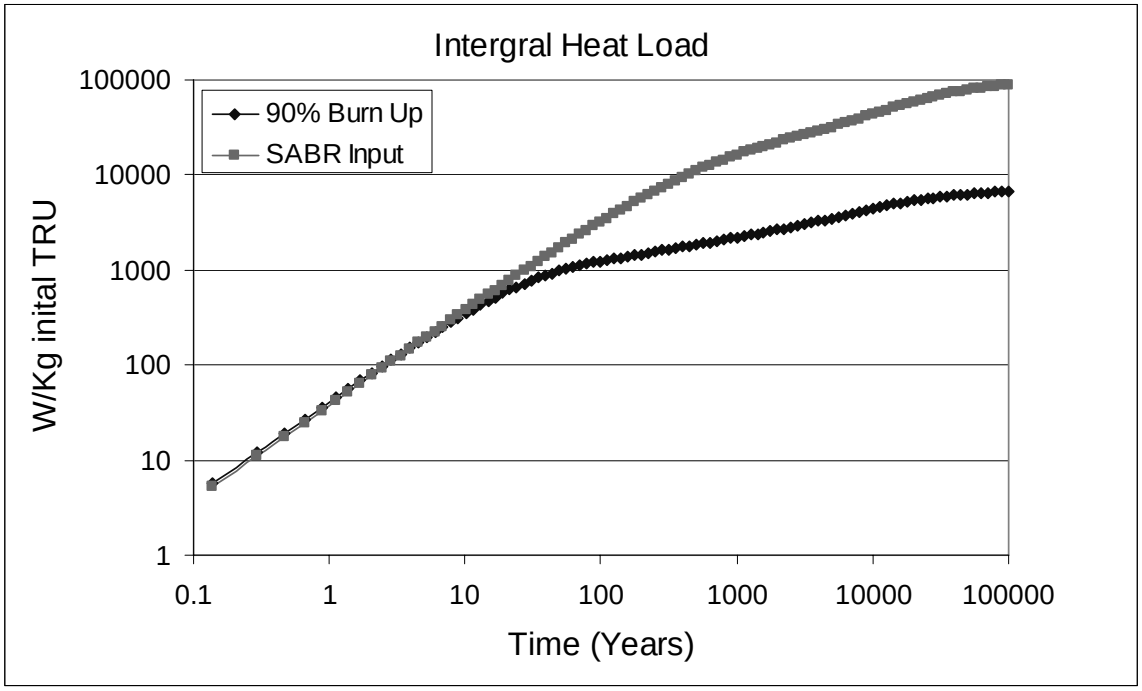

Figure 32: Integral Heat Load at 90% Burn Up for the Extended Burn Cycle

The 6834 W/kg of heat generated in this scenario is 13 times lower than the 88705 W/kg generated in the input fuel. This allows for a reduction in the required repository space by a factor of 13.

6.3.5 Summary of Extended Burn Cycle

Two assumptions were made for this scenario to operate. First, it was assumed that the materials could withstand a radiation damage limit of greater than 200 dpa. Secondly, the fusion neutron source strength was assumed to be stronger than the 500 MW that is currently designed. So even though this fuel cycle transmutes 91.2% of the transuranics and produces less integral decay heat. This cycle is currently not an option due to these constraints. In the future this cycle is not feasible due to the problems that exist with the power distribution. Approximately 2/3 of the power is being generated in the innermost fuel assembly. This creates large temperature gradients in the core resulting in unwanted mechanical defects. For this reason a deep burn of transuranics in a once through cycle is not feasible.

6.4 Scenario E: Reprocessing Fuel from SABR 3000 day fuel cycle

The objective of these calculations was to examine a scenario with TRU fuel reprocessing and recycling that could be used in the early stages of implementation of transmutation reactors (i.e. before an equilibrium fuel cycle involving a fleet of LWRs and ABRs was established). A 3000 day fuel cycle, limited by 200 dpa material damage to the clad and structure, with the out-to-in shuffling pattern was utilized for these calculations. The assumption that in the reprocessing stage 99% of the TRU is recovered and the reprocessed fuel is contaminated by 1% of the fission products initially present are used for the calculations in this scenario. The compositions of table 13 are taken at the end of cycle, no cool down time was assumed before reprocessing. The reprocessed fuel composition of table 13 is then admixed with fresh TRU. Enough fresh TRU is added so that 9 MT of fuel are loaded into the outer ring of the reactor. The fresh TRU that is admixed is the ANL fuel composition stated in section 2.3.

Table 13: Reprocessing Cycle Discharge Fuel Compositions

Isotope	Weight Percent
U-234	0.876
Np-237	12.722
Pu-238	10.625
Pu-239	27.325
Pu-240	23.28
Pu-241	3.445
Pu-242	4.703
Am-241	12.609
Am-242m	0.601
Am-243	2.818
Cm-244	0.787
Cm-245	0.103
*other	0.103

* The remaining fuel is composed of various U, Pu, and Cm isotopes

There is a 1 percent loss of TRU to the waste stream in the reprocessing. This one percent loss of TRU is used to calculate the decay heat to the repository. Table 14 summarizes the results for this scenario. The beginning of cycle k_{eff} of .900 is lower than in the non reprocessing cycle, this is due to a greater concentration of non fissile minor actinides being present in the fuel. This greater concentration of non fissile minor actinides in the fuel is due to transmutation of the minor actinides with high fission cross sections faster than the capture of minor actinides with low fission cross sections in previous cycles.

Table 14: Scenario E fuel cycle parameters

Parameter	Units	Values
Thermal Power	MW	3000
Cycles per Residence Time		4
Burn Cycle Length Time	Days	750
4 Batch Residence Time	Years	8.21
BOC keff		0.900
EOC keff		0.847
BOC Pfus	MW	181
EOC Pfus	MW	241
TRU BOC Loading	MT	36
Power Density	KW/kg	83.3
Power Peaking BOC		1.28
Power Peaking EOC		1.54
TRU Burned per Residence	%	23.6%
TRU Burned per Year	MT/FPY	1.03
TRU Burned per Residence	MT	8.496
SNF Disposed per Year	MT/FPY	103
LWR Support Ratio		4
Average Core Flux Across Cycle	n/cm^2-s	1.47E16
Average Fast (>0.1 MeV) Flux	n/cm^2-s	9.20E15
Fluence per Residence Time	n/cm^2	3.81E24
Fast Fluence per Residence Time	n/cm^2	5.75E15
Hardness of Spectrum	%	62.6%
Heat Load at 100,000 years	W/kg TRU Initial	.00187
Heat Load at 100,000 years SABR Input	W/kg TRU Initial	.127
Integral Heat Load	W/kg TRU Initial	667
Integral Heat Load SABR Input	W/kg TRU Initial	88705
Passes For 90% Burn Up	#	9
Reduction in Required Repository Space	Factor	129

The "core passes for 90% burn up", was calculated based on a single pass burnup calculation done in PERCOSET. The single pass burn is calculated using the FIMA equation (31), as fuel is recycled in the reactor it is assumed to experience the same destruction rate as the single pass burn up. Based off of this an accumulated burn up is calculated and the number of passes to reach 90% burn is calculated. Equation 40 was used to calculate the number of passes to 90% burn up:

$$100 * (1 - FIMA)^n \leq 10 \tag{40}$$

where n is the number of passes to achieve greater than 90% burn up.

The reduction in required repository space in this case is dependent on the separation of cesium and strontium from the rest of the fission products. Assuming 1% of the actinides are contained in the waste stream the required repository space is reduced by a factor of 129.

6.4.1 Power Profile

The power distribution for this scenario is quite similar to scenario C (Out-to-In shuffling same reflector configuration). The power distribution peaks more in this situation, power peaking of 1.28 and 1.54 for BOC and EOC respectively, compared to 1.12 and 1.31 for scenario C. This is caused by a less reactive fuel resulting in more neutrons being absorbed closer to the plasma. The power distribution for this cycle is shown in figure 33 below:

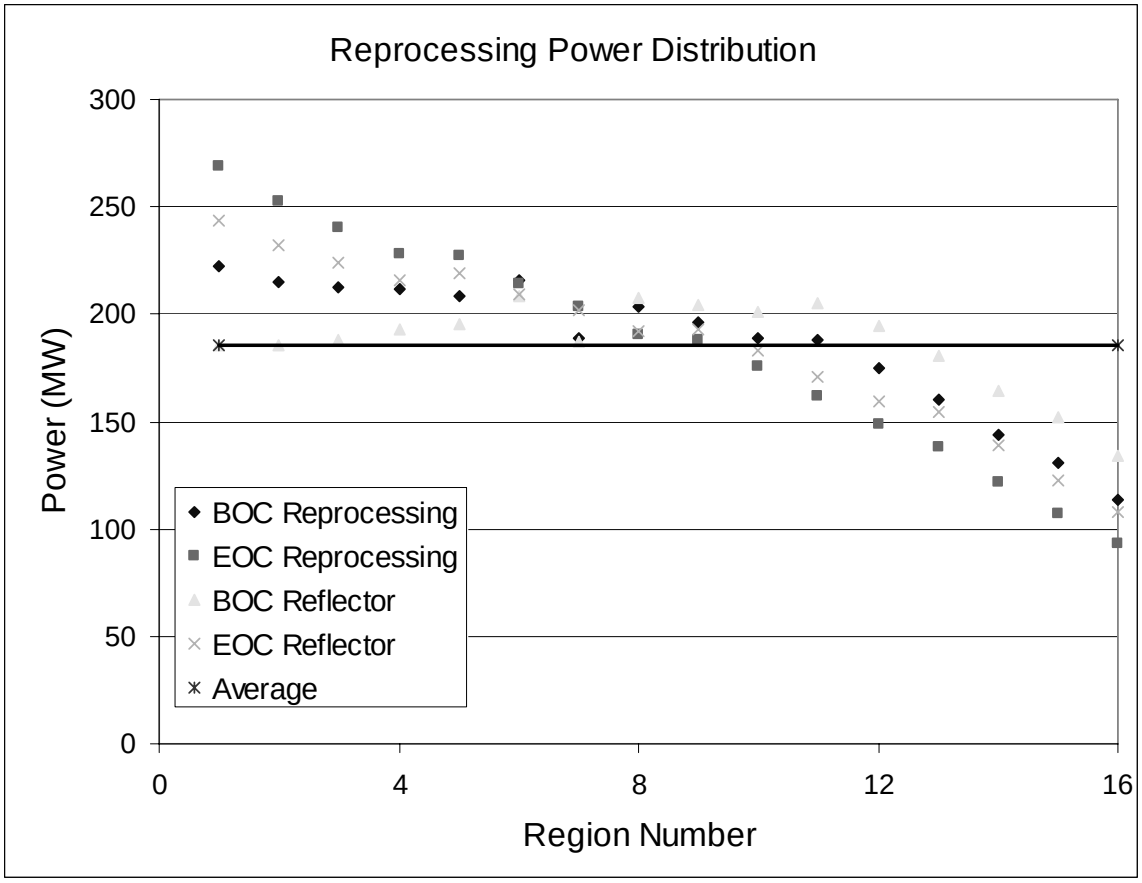

Figure 33: Reprocessing power distribution at BOC and EOC

6.4.2 Radiation Damage

The lower k_{eff} results in a higher fusion power and a softer spectrum than in scenario C (Out-to-In shuffling same reflector configuration). The softer spectrum can be seen in figure 34:

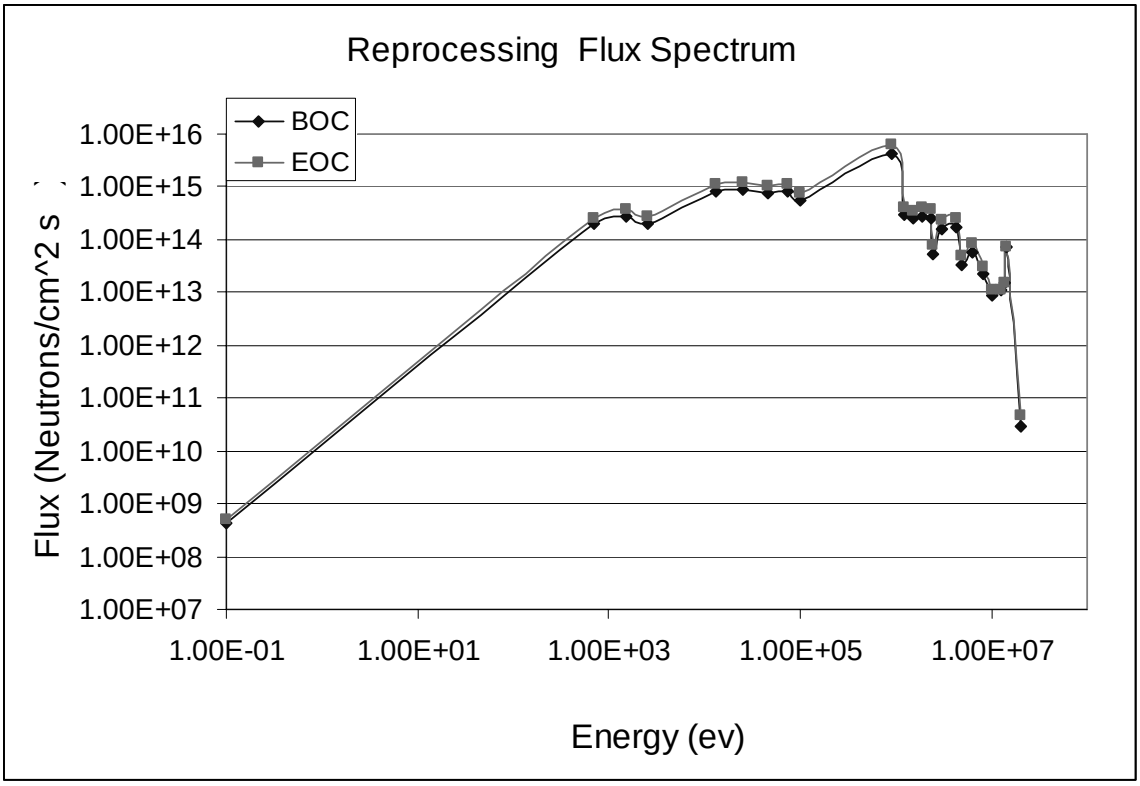

Figure 34: Reprocessing spectrum graph averaged over the entire core

6.4.3 Tritium Production

The calculation of tritium self sufficiency for this fuel resulted in missing self sufficiency by 1.5%. The beginning and end of cycle production and destruction rates are shown in table 15 below as well as the amount of tritium present at the beginning of the next cycle and the amount of tritium required for operation of the following cycle. This table was produced in the same manner as table 8 in section 6.1.3.

Table 15: Tritium Production

BOC Tritium Destruction	7.20e19 atoms/second
BOC Tritium Production	3.04e20 atoms/second
EOC Tritium Destruction	1.10e20 atoms/second
EOC Tritium Production	4.64e20 atoms/second
Tritium Necessary for BOC	6.89e21 atoms
Tritium at BOC	6.79e21 atoms

6.4.4 Heat load to the repository

The decay heat in this scenario is calculated based off of the TRU in the waste stream from the reprocessing plant. This is because the rest of the TRU is placed back into SABR to be transmuted. Using the reprocessing assumptions that 1% of the TRU are in the waste stream the decay heat curve and the integral heat curves are shown below:

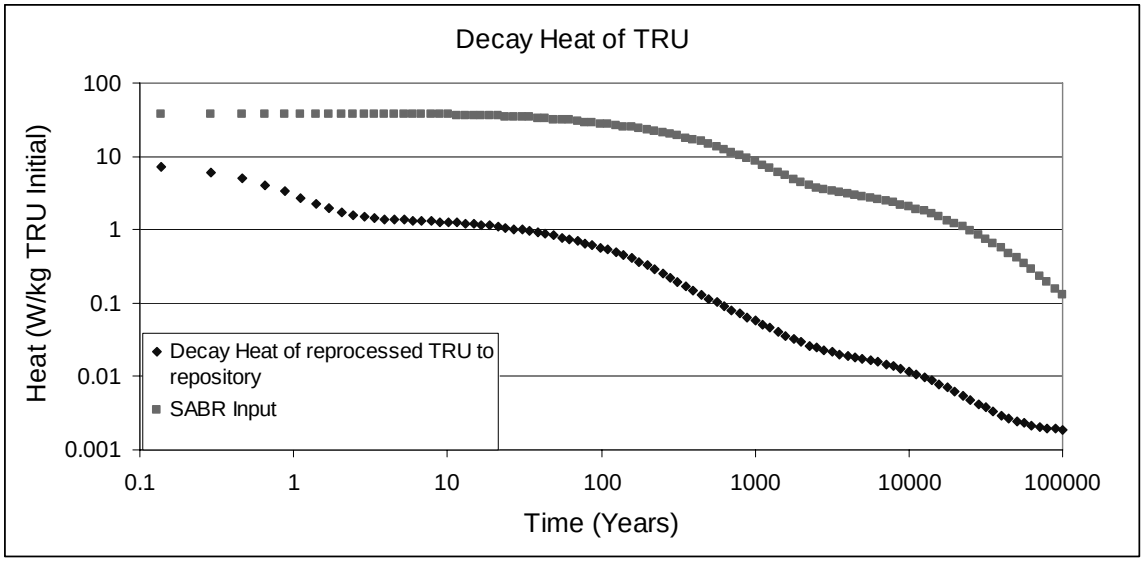

Figure 35: Decay Heat of Reprocessed Fuel to the repository

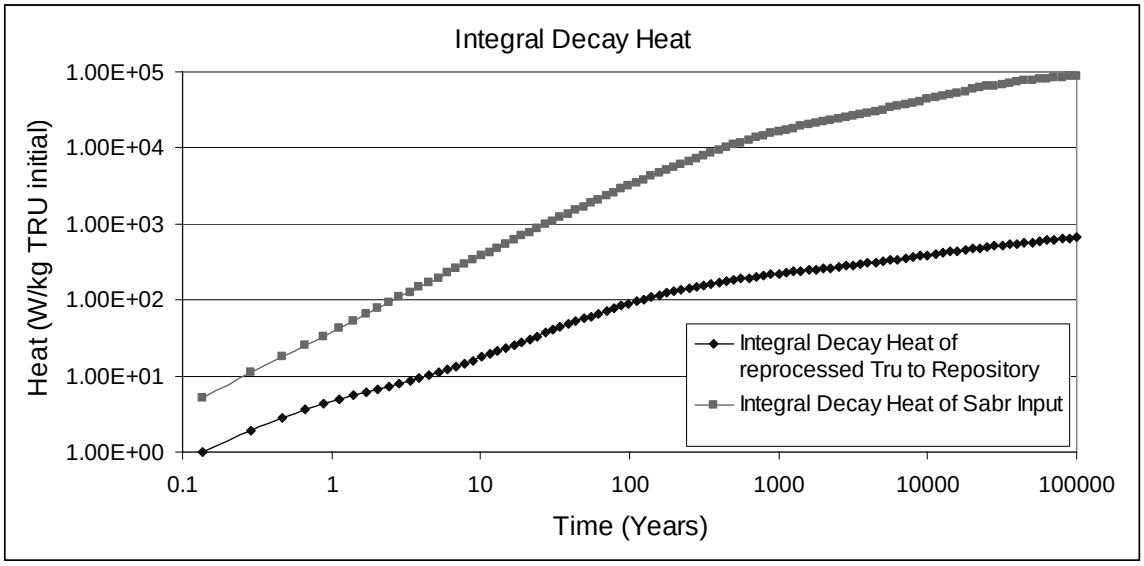

Figure 36: Integral Decay Heat of reprocessed fuel to the repository

The integral decay heat is much less in this scenario than in the extended burn scenario (scenario C) because only 1% of the TRU is being stored in the repository as opposed to 10% in the extended burn scenario. This results in a reduction of required repository space by a factor of 129 with the assumption that all of the cesium and strontium are removed and the other fission products are allowed to decay away for a few hundred years before being sent to the HLWR.

6.4.5 Summary of Reprocessing Fuel Cycle

The reprocessing and recycling fuel cycle is chosen as the reference cycle for SABR. This was chosen because it meets all of the design criteria. This fuel cycle had a relatively flat power distribution shown by the BOC power peaking factor of 1.28 and EOC power peaking of 1.54. It achieved a high transmutation rate and a burn up of greater than 90%. It was shown that tritium self sufficiency could be obtained by optimizing the breeding calculation and with the addition of a larger breeding blanket. The current configuration fell short by 1.5% but uses conservative assumptions. The long term decay heat from TRU was drastically reduced from about 48,000 W/kg to the repository, to a level of 677 W/kg to the repository. Finally, the reduction in required repository space was increased from a factor of 1.8 to a factor of 129.

Chapter 7: Conclusion

Two 4 batch fuel cycles were designed and analyzed with different shuffling patterns (in-to-out and out-to-in). Each of these cycles was limited by the fuel residence time of 3000 days due to radiation damage to structural materials. This residence time is limited by 200 dpa radiation damage accumulation and corresponds to a TRU burnup limit of less than 24% for SABR. The 24% fuel burnup destroyed 24% of the TRU as well as increases the amount of minor actinides with shorter half lives. This increase in the minor actinides with shorter half lives increases the initial decay heat of discharged fuel by a factor of 12 relative to SABR's input fuel, but it reduces the integral decay heat release over 100,000 years by a factor of 2. This was seen in both the in-to-out and out-to-in shuffling pattern. The out-to-in shuffling pattern was then chosen as the reference shuffling pattern because it had a more uniform power distribution over the burn cycle.

Next the configuration of the tritium breeding blanket and the reflector was examined in an effort to flatten the power distribution in the core. The fuel cycle calculation for the out-to-in cycle was repeated with a newly designed reflector (stainless steel followed by a layer of graphite) followed by the tritium breeding blanket. This design did flatten the power distribution while maintaining a 24% burnup of the TRU. This design also allowed for SABR to maintain self sufficiency by breeding enough tritium over the cycle to operate the fusion neutron source.

A third fuel cycle examined was an extended cycle that achieved 90% burnup of the TRU in a once through cycle (without reprocessing/recycling). This 4 batch cycle could be considered if new structural materials are developed that can withstand the radiation damage associated with this extended cycle. This scenario would require minor modifications to the fusion neutron source to accommodate the low k_{eff} at the end of cycle. However, the major issue with this extended cycle is the non-uniform power distribution, which was exponentially attenuated with distance from the fusion neutron source.

Finally, a 4 batch fuel cycle representative of the ABR's fuel cycle envisioned by GNEP was explored. This 4 batch, 3000 day cycle with repeated reprocessing and recycling of the TRU fuel to achieve greater than 90% burnup of the fuel after 9 recycles. The decay heat to the repository in this cycle would be short term and caused by the fission products. The reduction in necessary repository space by a factor of 129 is due to only 1% of the TRU having to be placed in the repository. This fuel cycle is the reference cycle for SABR. It was chosen as the reference

cycle, because it meets all of the design criteria: 1) minimizes power peaking, 2) achieves a high transmutation rate and reaches 90% burnup of the TRU, 3) produces enough tritium to maintain self sufficiency, 4) decreases the long term decay heat, 5) and it reduces the repository requirements for spent nuclear fuel by a factor of 129.

This study shows that to make a considerable impact on repository space a reprocessing and recycling fuel cycle is necessary. A once through cycle that burns 90% of the TRU, if possible, is not enough to make a considerable impact on the repository space. This study showed that a once through cycle at 90% burnup increases the repository space by a factor of 13. When the recycling and reprocessing cycle was analyzed 1% of the TRU had to be stored in the repository and the reduction in repository space increased by a factor of 129. A reprocessing and recycling fuel cycle can cause a greater gain in repository space if the separations technology in reprocessing is enhanced. The less contaminated the waste stream is with TRU the greater increase in repository space. To achieve the greatest increase in repository space SABR would need to operate with reprocessing and recycling. The reprocessing fuel cycle currently envisioned by SABR increases the space of Yucca Mountain by a factor of 129 this equates to a new repository being needed every 4515 years instead of every 70 years.

References

1. Office of Civilian Radioactive Waste Management http://www.ocrwm.gov

2. J. Russel, et al., Rethinking the Challenge of High Level Nuclear Waste: Strategic Planning for Defense High-Level Waste and Spent Fuel Disposal, (May 2007)

3. P. Lisowski, Global Nuclear Energy Partnership, Presentation to GNEP Annual Meeting, (October 2, 2007).

4. N.D. Rosenberg, G.E. Gdowski, K.G. Knauss, "Evaporative chemical evolution of natural waters at Yucca Mountain, Nevada", *Applied Geochemistry*, (2001).

5. Argonne National Lab http://www.anl.gov

6. G.R. Choppin, J. Liljenzin, J. Rydberg. *Radiochemistry and Nuclear Chemistry.* Butterworth-Heinemann Ltd, 1995.

7. DoE Global Nuclear Energy Partnership website http://www.gnep.energy.gov

8. Nuclear Regulatory Commision website http://www.nrc.gov

9. O.H. Zabunoglu, L. Ozdemir, "Purex co-processing of spent LWR fuels: flow sheet"; *Annals of Nuclear Energy,* (2005).

10.G.F Vandegrift et al., "Designing and Demonstration of the UREX+ Process Using Spent Nuclear Fuel", *ATATLANTE 2004* (June 2004).

11. Global Nuclear Energy Partnership Technology Development Plan (July 2005).

12. W. M. STACEY, et al., "A TRU-Zr Metal Fuel, Sodium Cooled, Fast Subcritical Advanced Burner Reactor", *Nucl. Technol.*, 162, 53 (2008).

13. International Thermonuclear Experimental Reactor http://www.iter.org.

14. K. E. ABNEY, et al. Advanced Nuclear Fuel Processing Options Final Report, Los Alamos National Laboratory. (Oct. 6, 1997).

15. Personal Communication Stephen Hayes and Mitchell Meyer, Argonne National Laboratory (2007).

16. G. F.MAUER,, Design and Evaluation of Processes for Transmuter Fuel Fabrication, Report. University of Nevada Las Vegas. (August 2001)

17. G. F. MAUER, Design and Evaluation of Processed for Fuel Fabrication: Quarterly Progress Report #3, University of Las Vegas Nevada. (March 1, 2002).

18. F. VON HIPPELl, Managing Spent Fuel in the United States: The Illogical of Reprocessing, <www.fissilematerials.org> (Jan. 2007).

19. M. K. MEYER, et al. Development and Testing of Metallic Fuels With High Minor Actinide Content, Argonne National Laboratory, Idaho Falls, Idaho. April 20, 2003.

20. 2002 Research Highlights: Technology Pioneered at Argonne Shows Promise For Next Generation of Nuclear Reactors. (April 23, 2007). http://www.anl.gov/Media_Center/Frontiers/2002/d1ee.html
21. D. BODANSKY, "Reprocessing spent nuclear fuel." Physics Today. 80-81. (Dec., 2006).
22. K. W. BUDLONG-SILVESTER, K.W., J. F. PILAT,, Safegaurds and Advanced Nuclear Energy Systems: Enhancing Safeguardability. Los Alamos National Laboratory. (Oct. 14, 2003).
23. Report on the Preferred Treatment Plan for EBR-II Sodium Bonded Spent Nuclear Fuel. Office of Nuclear Energy, Science and Technology, U.S. Department of Energy. (October, 2003).
24. Pyrochemical Separations in Nuclear Applications: A Status Report. Nuclear Energy Agency, Organisation for Economic Co-operation and Development. (2004).
25. D. C. CRAWFORD, S.L. HAYES, M.K. MEYER, Current US Plans For Development of Fuels for Accelerator Transmutation of Waste. Argonne National Laboratory, Idaho Falls, Idaho.
26. W. M. STACEY, et al., "Advances in the Subcritical Gas-Cooled, Fast Transmutation Reactor Concept", *Nucl. Technol.*, (July, 2007).
27. "Javapeno," NUREG/CR-200, Vol. III Section M20, ORNL/NUREG/CSD-2/R7 (2006).
28. "Triton: A Two-Dimensional Depletion Sequence for Characterization of Spent Nuclear Fuel," NUREG/CR-200, Rev. 5., Vol. I Section T1, ORNL/NUREG/CSD-2/R7 (2006).
29. "NEWT: A New Transport Algorithm For Two-Dimensional Discrete Ordinates Anaylsis In Non-Orthogonal Geometries," NUREG/CR-200, Rev. 5.1, Vol. II Section F21, ORNL/NUREG/CSD-2/R7 (2006).
30. "SCALE5.1: A Modular Code System for Performing Standardized Computer Analyses for Licensing Evaluation," NUREG/CR-0200, Rev. 5.1 (ORNL/NUREG/CSD-2/R5), Vold. I, II, and III, Oak Ridge National Laboratory/U.S. Nuclear Regulatory Commission (2006).
31. C. de OLIVEIRA and A.GODDARD, "EVENT—A Multi-dimensional Finite Element Spherical-Harmonics Radiation Transport Code," Proc. Int. Seminar *3-D Deterministic Radiation Transport Codes*, Paris, France, December 2–3, 1996, Organization for Economic Cooperation and Development (1996).
32. R.E. MACFARLANE & D.W. MUIR. "The NJOY Nuclear Data Processing System, Version 99," Los Alamos National Laboratory (1999).
33. J.W. Maddox, "Fuel Cycle Optimization of a Helium-Cooled, Sub-Critical, Fast Transmutation of Waste Reactor with a Fusion Neutron Source", MS Thesis, Georgia

Institute of Technology, (May 2006); also J. W. Maddox and W. M. Stacey, "Fuel Cycle Analysis of a Subcritical Fast Helium-Cooled Transmutation Reactor with a Fusion Neutron Source", Nucl. Technol., 158, 94 (2007).
34. "User's Guide for AMPX Utility Modules," NUREG/CR-200, Vol. III Section M15, ORNL/NUREG/CSD-2/R7 (2006).
35. F. Goldner, R Versluis, "Transmutation Capabilities of Gen-IV Reactors" (September 2006).
36. J. P. Floyd, et al., "Tokamak Fusion Neutron Source for a Fast Transmutation Reactor", Fusion Sci. Technol., 52, 727 (2007).